AN ABSTRACT OF THE THESIS OF

RICHARD ALLEN DOWNS for the degree of Master of Ocean Engineering

in Ocean Engineering presented on June 10, 1976

Title: FLOWS ASSOCIATED WITH HARBOR SHIP TRAFFIC

Abstract approved: Redacted for Privacy

The purpose of this study was to ascertain the potential erosion impacts associated with ship movements in confined waters. The flow associated with a ship passage can be separated accordingly: (1) the propeller wake, (2) flow about the hull, and (3) associated waves. Each of these areas has been analyzed to determine their respective potential for causing channel erosion.

Extensive field work was planned to determine the magnitude of the associated flows in a channel due to a ship passage, but numerous problems developed that limited the amount of useful data obtained. As an alternative approach, use was made of data presented by other authors concerning channel flow effects caused by a ship passage. SOGREAH test results regarding Kiel Canal flows and ship related disturbances (Wasser-und Schiffahrtsdirektion Kiel, 1966) appear to be particularly applicable for the Coos Bay shipping channel because the channel dimensions and ship sizes in the two areas are approximately equal. From the Coos Bay field work that was completed and from the extrapolations of the SOGREAH test results, the total erosion caused by ship traffic in Coos Bay was estimated to be insignificant compared to the natural erosion and deposition that takes place in the estuary.

# Flows Associated with Harbor Ship Traffic

by

Richard Allen Downs

A THESIS

submitted to

Oregon State University

in partial fulfillment of
the requirements for the
degree of

Master of Ocean Engineering

June 1977

APPROVED:

Redacted for Privacy

Professor of Civil Engineering
in charge of major

Redacted for Privacy

Head of Department of Civil Engineering

Redacted for Privacy

Dean of Graduate School

Date of thesis presentation June 10, 1976

Typed by Janice Carleton for RICHARD ALLEN DOWNS

ACKNOWLEDGEMENTS

This investigation was made possible by funding from the National Science Foundation - Research Applied to the Nation's Needs. Special thanks is given for the advice and encouragement of Dr. Larry Slotta who served as major professor. Additional help has been obtained from Dr. R.T. Hudspeth, Dr. C.K. Sollitt, Bob Arneson, Dixie and Scott Boley, Janice Carleton, Steve Crane, Larry Crawford, Greg Hartman, Steve Klein, Esther Newman, and Cara Pence. I would also like to thank the U.S. Army Corps of Engineers for their help and the use of their facilities at Coos Bay and the Bundesanstalt Fur Wasserbau and the Delft Hydraulics Laboratory for sharing their information on ship traffic in canals. Most of all I want to thank my family for always being behind me in everything I have chosen to do and my friends at the University of Minnesota who I have thought of often over the last two years.

TABLE OF CONTENTS

LIST OF FIGURES

LIST OF FIGURES (cont.)

LIST OF TABLES

## LIST OF SYMBOLS

| Symbol | | Dimension |
|---|---|---|
| A | maximum wetted cross sectional area of ship | $L^2$ |
| $A_0$ | circular area of propeller disc | $L^2$ |
| AP | stern of ship | - |
| B | maximum width of ship at waterline | L |
| $B_0$ | the beam of a ship divided by $\varepsilon$ | L |
| b | length of a propeller blade | L |
| c | constant spread coefficient | - |
| D | diameter of jet nozzle | L |
| $D_1$ | draft of ship | L |
| d | dimensionless squat, $h-h_1/h$ | - |
| E | energy | $mL^2/T^2$ |
| $E_r$ | erosion rate | $L^3/L$ |
| $F_a$ | cross sectional area of canal | $L^2$ |
| F | Froude number based on water depth | - |
| FP | bow of ship | - |
| $F_L$ | Froude number based on ship length | - |
| f | function describing a ship hull | L |
| g | gravitational constant, 9.8 $m/sec^2$ | $L/T^2$ |
| H | wave height | L |
| h | water depth | L |
| $h_1$ | water depth alongside a ship | L |
| $h_0$ | water depth divided by $\varepsilon$ | L |
| i | unit vector in x direction | - |
| j | unit vector in y direction | - |

## LIST OF SYMBOLS (cont.)

| Symbol | | Dimension |
|---|---|---|
| k | unit vector in z direction | - |
| L | one half of a ship's length | L |
| $\ell$ | crest length of a wave | L |
| m | number of propeller blades | - |
| n | passage coefficient, F/A = 1/S | - |
| r | radial distance | L |
| S | blockage coefficient (1/n) | - |
| $S_a$ | cross sectional area of hull below waterline | $L^2$ |
| $S_a'$ | derivative of cross sectional area of hull | L |
| T | thrust | $mL/T^2$ |
| U | free stream current velocity | L/T |
| $U_0$ | velocity of water leaving propeller on jet nozzle | L/T |
| $\overline{(U^2)}_0$ | average of the square of the velocity leaving the jet nozzle | $L^2/T^2$ |
| $U_c$ | velocity at centerline of jet | L/T |
| u | velocity component in X direction | L/T |
| V | current velocity | L/T |
| $\overline{V^2}$ | average of the square of the current velocity | $L^2/T^2$ |
| $V_{r_m}$ | mean speed of the return current | L/T |
| $V_s$ | ship velocity | L/T |
| $V_{s_{max}}$ | maximum ship velocity | L/T |
| $v_\theta$ | tangential velocity induced by vortices | L/T |
| WL | water level | - |
| x | coordinate in direction of propeller axis | L |
| y | lateral or horizontal coordinate | L |

LIST OF SYMBOLS (cont.)

| Symbol | | Dimension |
|---|---|---|
| $z$ | vertical coordinate, origin at free surface | L |
| $z_0$ | depth of the center of jet nozzle | L |
| $\Gamma$ | circulation density | $L^2/T$ |
| $\gamma$ | specific weight of water | $F/L^3$ |
| $\epsilon$ | small parameter or perturbation | - |
| $\eta$ | elevation of the free surface | L |
| $\lambda$ | wave length | L |
| $\xi$ | dummy variable | - |
| $\rho$ | density of water | $m/L^3$ |
| $\phi$ | velocity potential | - |
| $\omega$ | angular velocity of propeller | $T^{-1}$ |
| $\nabla$ | differential operator $\frac{\partial}{\partial x} i + \frac{\partial}{\partial y} j + \frac{\partial}{\partial z} k$ | - |

# FLOWS ASSOCIATED WITH HARBOR SHIP TRAFFIC

## I. INTRODUCTION

The size of ships have continued to increase so that many waterways are now being used by large vessels that can scarcely navigate through the shipping canals safely. When a large ship operates in confined waters, in close proximity to the bottom or canal banks, a change in the current velocity in parts of the canal is effected. This velocity increase can be large enough to cause significant erosion of the canal sediments (Schiffbau, 1912; Delft, 1974).

The purpose of this study was to describe the flows associated with a ship moving in confined waters and to estimate the erosion caused by ship traffic in a canal. The disturbance of the water in a canal due to the movement of a ship can be divided into three areas: the flow caused by the ship propeller, the ship hull, and ship waves. Each of these areas have been analyzed to determine the respective potential for causing canal erosion. SOGREAH test results (Wasser und Schiffahrtsdirektion Kiel, 1966) have been used to estimate the total erosion in a canal caused by ship traffic.

## II. SHIP MOVEMENT IN CANALS

When a ship operates in confined waters, the ship influences the flow field around it and in return is acted upon by sizeable hydrodynamic forces created by the flow field. A vessel in a canal changes the flow field in three different ways. (1) Due to the presence of the hull, there is a decrease in area through which the water can flow and hence there is an increase in the current velocity. (2) The propeller adds energy to the water and causes an increase in velocity in the wake of a ship. (3) Ship waves transport energy away from a ship and dissipitate that energy on the shore. The flows associated with a ship hull, ship propeller, and ship waves will be investigated after two important forces acting on a ship are discussed.

### Squat

One force that can be of major concern is that which causes a ship to sink or squat in the water when underway. Squat occurs due to an increase in water velocity and a decrease in pressure beneath a ship. The increase in water velocity can be caused by either the propeller drawing water from beneath the stern, or the increased flow due to a constriction in area beneath the ship. Squat has been found to be a function of: (1) ship speed; (2) depth of water; (3) width and cross-section of the canal; and (4) wetted cross-section of the vessel (Kray, 1970; Waugh, 1971). Figure 1 (Constantine, 1960) shows the relationship between Froude number and the dimensionless squat of a ship for various values of the blockage coefficient, S, the ratio of

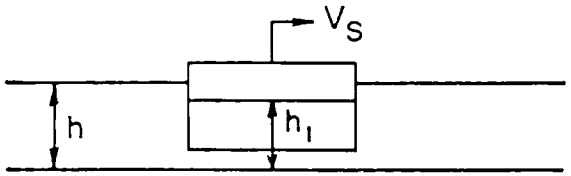


$$d = \frac{h - h_1}{h}$$

$$F = \frac{V_S}{\sqrt{g\,h}}$$

$$S = \frac{\text{ship cross-sectional area}}{\text{canal cross-sectional area}}$$

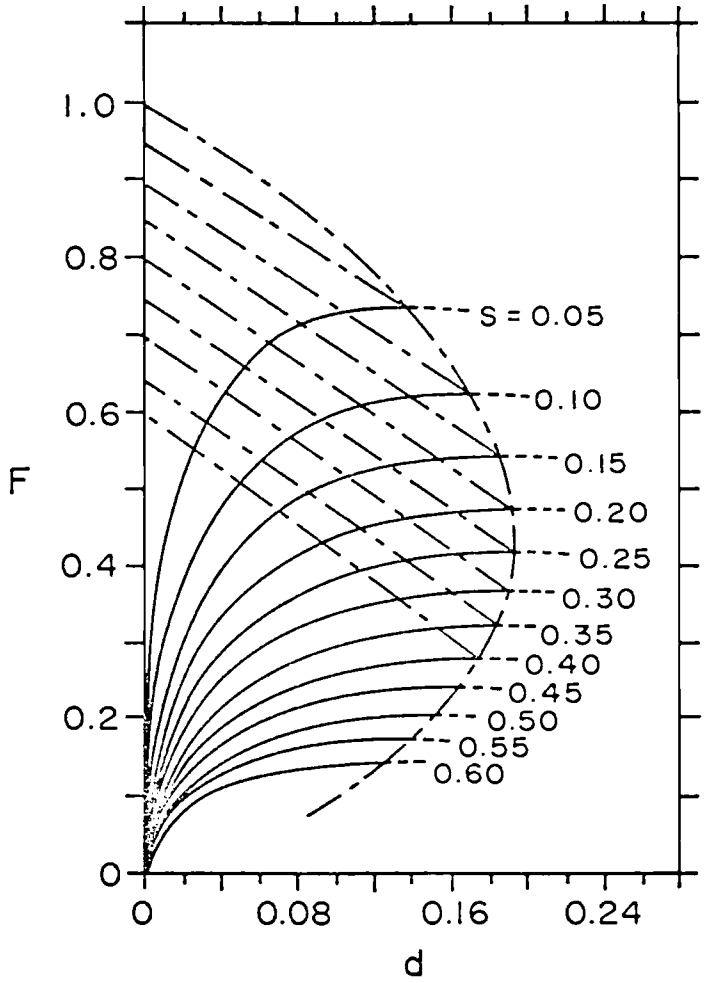


Figure 1. Relationship between the Froude number F (based on the speed of the ship and the undisturbed depth of the canal) and the dimensionless squat d of the ship for various values of the blockage coefficient S. (From Constantine, 1960)

maximum wetted cross-sectional area of a ship to the canal cross-sectional area. Where a dredged channel depth only slightly exceeds the natural depth over a wide bay, squat might be practically insignificant at normal operating speeds. Conversely, a dredged channel located in a normally shallow estuary might reflect squat measurements similar to those experienced in canals of limited dimensions (Waugh, 1971). Squat is sufficiently important to be considered for operations in many canals because grounding of ships or erosion of the banks due to excessive ship waves can occur.

Limiting Speed

Other forces acting on vessels limit their maximum speed at which they travel in a canal. When a ship moves under the action of its propeller, water is drawn through the plane of the propeller at a rate depending upon the shaft rotational speed and the available engine power. The corresponding rate of change of momentum is opposed by a reacting thrust which causes the ship to accelerate until it attains a steady speed. In open water the ship's acceleration is accomplished simply by increasing the propeller's rotational speed. Accordingly, more water is drawn through the propeller and thus the impulsive force increases. This flow rate might be expected to continue to increase to an amount limited only by the engine power and the performance of the propeller. Acceleration could continue to the physical limits imposed by the engine and propeller since nothing prevents an abundant supply of water from entering the propeller.

Similar acceleration effects would initially be experienced in

restricted waters while the vessel accelerates from rest; but in these circumstances other factors would begin to influence the flow rate into the propeller. The thrust from the propeller reaches a limiting value simultaneously with the maximum ship speed, since the thrust depends on backflow discharge, and this limiting thrust remains steady so long as ship speed remains at the maximum speed. Therefore, it would seem that by increasing the propeller's rotational rate, more water could be drawn through the propeller and the thrust would further increase. This does not occur though, because the propeller operates in a region of critical flow in which the volume of water drawn through the propeller becomes limited and cannot increase, regardless of the increased revolutions of the propeller. It follows that thrust cannot increase because the propeller has become starved of water, thus ship speed remains steady, or sometimes actually decreases, irrespective of any increased propeller rotation. The principal parameter which appears to control this speed is the blockage coefficient, S (Schofield, 1974).

In the Kriegenbrunner Survey (1975) it was also recognized that a ship has a maximum speed in a canal. Tests showed the following relation approximated the maximum ship velocity in a canal.

$$V_{s_{max}} = 1.5n + 1 \qquad (1)$$

where n, the ratio of the cross-sectional area of the canal to the maximum cross-sectional area of the ship, is the inverse of S, the blockage coefficient, and $V_{s_{max}}$ is the maximum ship velocity represented in km/hr. When propeller rotational rates were increased be-

yond the value where $V_{s_{max}}$ first appeared, there was no increase in ship velocity, but an increase in the scour of the canal floor was observed. Equation (1) has not been tested in different size canals, so its applicability over a wide range of canals is not known.

## III. PROPELLER WAKE

A ship wake is defined as the disturbance of the water following passage of a ship. Three major components of a wake include: water being pushed backward alongside the hull, dragged along behind the hull, or pushed astern by the propeller. The water pushed backwards alongside the hull follows the shape of the hull, and near the stern the water moves upward due to the narrowing of the ship. Figure 2 (Namimatsu and Muraoka, 1974) shows the flow beginning a short distance in front of the stern for one particular ship. The flow in front of the stern of most ships underway can be expected to be similar to the flow in Figure 2, but the exact flow pattern will depend on the form of the ship near the stern.

A ship's wake is primarily due to the propeller. The water in the outflow jet of a propeller has a rotational velocity component in addition to an axial velocity component. A propeller jet is unusual among submerged liquid jets in that the jet maintains its identity for many propeller diameters downstream. The distance that the propeller wake persists depends on the type of ship and its speed. Axial velocities have been observed to persist for distances extending from 5 to 15 propeller diameters behind the ship, while there have been traces of the rotational velocities 24 diameters beyond the ship's propeller (Saunders, 1957).

Besides knowing the distance a propeller wake persists, it is important to know where the wake travels after leaving the propeller. From studies conducted with a destroyer model, Saunders (1957) found

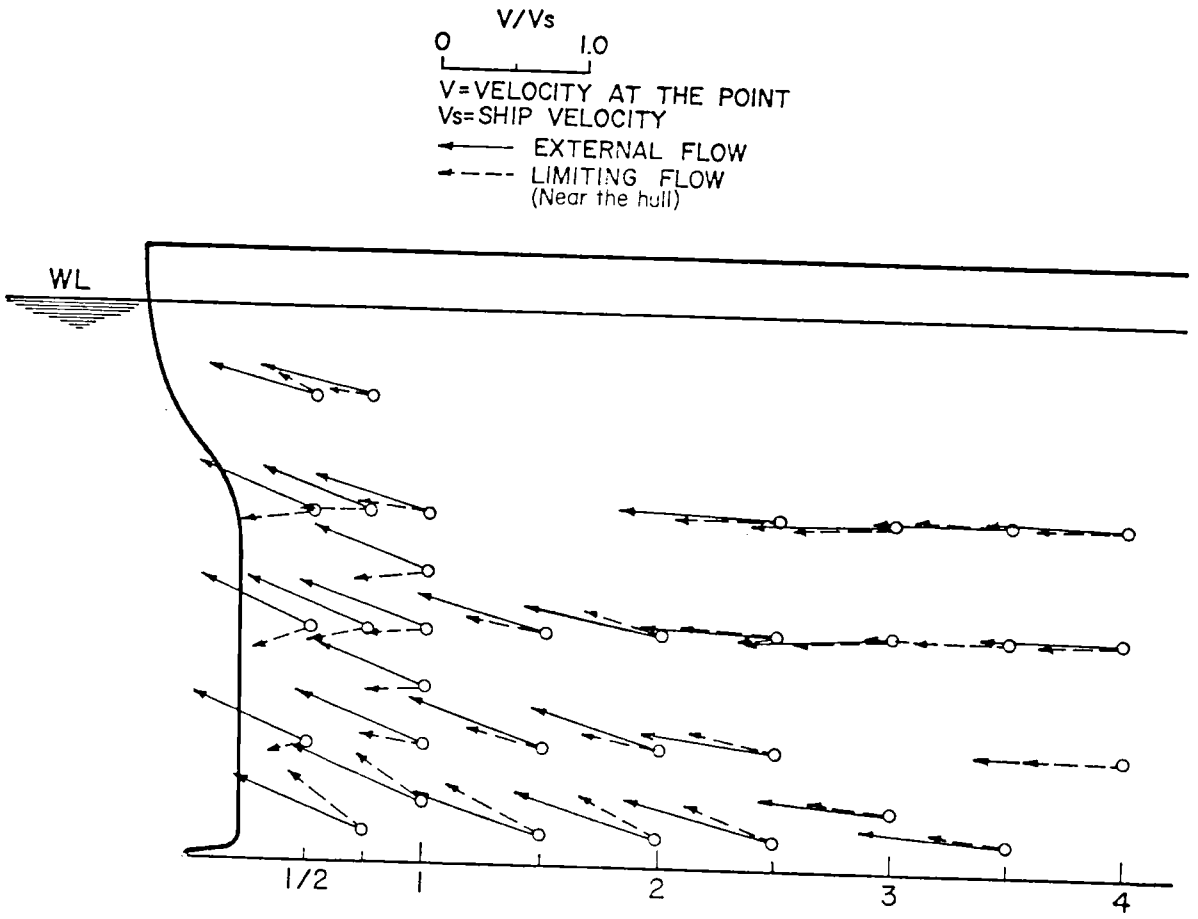


Figure 2. Flow field near a ship hull in proximity to the stern. (From Namimatsu and Muraroka, 1974)

that the longitudinal centerline of the outflow jet does not lie along an extension of the propeller shaft axis. Instead, it begins to rise just behind the propeller, where the outflow jet coincided with the rise in the water flowing under the stern. Because of the lack of other observations in the upper portions of the propeller outflow jet, it was difficult to estimate the limits and shape of the cone of diffusion between the outflow jet and the surrounding waters (Saunders, 1957).

One method recently used for obtaining the diffusion of the outflow jet has been through aerial photography. Aerial photographs taken of towboats and barges on the Illinois River (Karaki and van Hoften, 1975) show the spread of the ship's wake on the surface, but the pictures give no indication of the diffusion of the wake below the surface. A more accurate determination of the wake can be made by looking at the acoustic wake produced by a ship.

An acoustic wake is defined as a volume of water which has a greater capacity for absorbing and scattering sound after a ship has passed through it (Physics of Sound in the Sea, 1969, p. 441). An acoustic wake is formed by air that is trapped along the waterline of a vessel and then dispersed in the form of bubbles, or from air bubbles that are formed by the propeller. From the manner in which an acoustic wake is formed, it is believed that a ship's "normal" wake and acoustic wake coincide.

The width of a ship's acoustic wake has been found to increase with distance behind a ship. At distances greater than 100 yards, the wake behind destroyer and destroyer escorts were observed to fan

out laterally, with the edges of the wake including a total angle of 1° (Physics of Sound in the Sea, 1969, p. 494).

The formation of wakes is apparently affected by the wind direction. The thickness of an acoustic wake has been found to vary behind the same vessel run at the same speed in different directions. In some cases the thickness of the wake was the same along the width, while in other cases the wake was thinner at the edges. The wake thickness for large surface vessels has been reported to be approximately twice the draft of the vessel, with the wake being approximately constant in thickness up to distances of 900 m behind the ship (Physics of Sound in the Sea, 1969, pp. 498-500).

A propeller wake can also be observed with a side scan sonar if there is enough sediment suspended in the wake to reflect the signal from the transducer. Hartman (1976) used an E.G.&G. Side Scan Sonar to detect the propeller wake behind the Hopper Dredge HARDING while it was dredging in Coos Bay, Oregon. The quantity of suspended sediment in the wake was great enough to completely block the signal from the transducer and keep it from recording any features on the far side of the wake. At a distance of approximately 200 m past the vessel the suspended sediment in the wake was dispersed enough so that a normal view of the channel was obtained. This indicates that there is a rapid dispersion of suspended sediments behind a vessel due to the turbulence in a propeller wake.

In the Kriegenbrunner Survey (1973) the actual wake behind a ship has been found to be much smaller than the size of the wake predicted from the acoustic wake study (Physics of Sound in the Sea, 1969). In

the Kriegenbrunner Survey two different types of vessels were used in the tests; one a motor freight ship, the other a tugboat which was pushing a barge.[1] Five passes by a freight ship, having a draft of 2.3 meters, were made over the test area at three water depths: 4.0, 3.5, and 3.1 meters. Only once during the 15 runs was the propeller wake noticeable on the bottom. Conversely, the propeller wake of the tug boat, having a draft of 1.65 meters, reached the bottom in 11 out of 13 runs at four different water depths: 4.0, 3.5, 3.1, and 2.8 meters. These field tests with large vessels indicate that the thickness of a propeller wake is a highly variable quantity and depends to some extent on the size, pitch and revolution speed of the vessel's propeller, and particularly the draft of the ship.

When a propeller wake extends to the bottom, the wake can cause a considerable amount of scour. Shortly after the completion of a number of canals in Germany, the harmful effects of propeller wakes on canal beds were observed (Schiffbau, 1912). It was discovered that ships caused the eroding of sediments in the center of the canal with subsequent deposition taking place along the sides. The volume of sediment settling along the canal's sides would build up to make it impossible for two ships to pass in what was originally a two-way canal. Model tests of operations of various sized ships were conducted to determine what parameters were important in causing the scour. It was determined that rudder orientation had the greatest influence

---

[1]Physical dimensions of the vessels are listed in the Appendix.

on the scour. As the circular component of velocity in the propeller wake struck the rudder it would subsequently be deflected downward. The amount of scour caused by the deflected jet was considerable, as listed in Table I from the early German studies.

To determine the amount of scour caused by a propeller wake, the ship GUSTAV KOENIGS, having a draft of 2.0 meters,[2] was anchored in a canal which had a protective layer 1.5 meters deep consisting of stones six to ten centimeters in diameter (Felkel and Steinweller, 1972). The vessel was anchored and its propeller was run for 30 minutes with a bottom clearance of: 1.0, .78, .71 and .28 meters. At the end of each test a depression was created behind the propeller with a mound deposited beyond the depression. Figure 3 shows the relation between the scour depth and mount height as a function of the bottom clearance. Figure 4 shows the volume of material scoured as a function of the bottom clearance. For the type ship used in this test it was decided that a minimum bottom clearance of 1.0 meters was needed to keep scour to a minimum. Figures 5 and 6 show the chronological development of scour with time for a different set of tests. After the propeller had run for only five minutes, the scour depth attained 3/4 of the value reached after 50 minutes. This indicates that if a ship is in close proximity to the bottom, the propeller wake can cause an appreciable amount of scour while the ship is just getting underway.

Field measurements of scour caused by a moving ship were also made

---

[2]Additional information on the ship is listed in the Appendix.

TABLE I. RESULTS OF PROPELLER TESTS (Schiffbau, 1912)

| Name of the Vessel | Draft m | Propeller Diameter m | Thrust During Test in Kg | Number of Revolutions of the Propeller per Minute | Maximum Scour With Rudder m | Maximum Scour Without Rudder |
|---|---|---|---|---|---|---|
| Water depth: 5.2 m | | | | | | |
| | | | a) Single Propeller Tugboat | | | |
| " FRIEDEFÜRST | 1.27 | 1.20 | 1200 | 200 | .40 | --- |
| HELGOLAND | 1.34 | 1.10 | 1000 | --- | 1.60 | .20 |
| FRIEDRICH WILHELM | 1.28 | 1.23 | 1200 | 200 | 1.40 | .10 |
| GUSTCHEN | ---- | 1.35 | 1200 | 220 | .30 | .60 |
| ELFRIEDE | 1.40 | ---- | 850 | 180 | 1.60 | --- |
| ALFRED | 1.35 | 1.15 | 950 | 190 | .45 | --- |
| | | | b) Tugboat with Twin-Propellers | | | |
| RHEIN | 1.24 | ---- | 1200 | 125-120 | .1 | --- |
| ANNA | 1.12 | .95 | 1000 | 210 | 1.40 | --- |
| ANNA | 1.12 | .95 | 460 | 130 | .40 | --- |
| ANNA | 1.12 | .95 | 1200 | 100 | .60 | --- |
| ANNA | 1.12 | .95 | 1600 | 134 | .40 | --- |
| GOEBEN | 1.56 | 1.30 | 2100 | 160 | .30 | --- |
| | | | c) Tugboat with Tunnel Stern | | | |
| KLARA | 1.15 | 1.48 | 1200-1250 | --- | .3 | --- |
| KLARA | 1.15 | 1.48 | 1700-1750 | --- | .6 | --- |
| KLARA | 1.15 | 1.48 | 1700-1750 | --- | .9 | --- |
| KLARA | 1.15 | 1.48 | 2600 | --- | 1.0 | --- |
| | | | d) Freight Steamer | | | |
| FALK | 1.36 | 1.35 | 1200 | 210 | .10 | --- |
| | | | e) Cruise Ship | | | |
| " GLÜCKAUF | 1.20 | 1.20 | 925 | --- | .10 | --- |

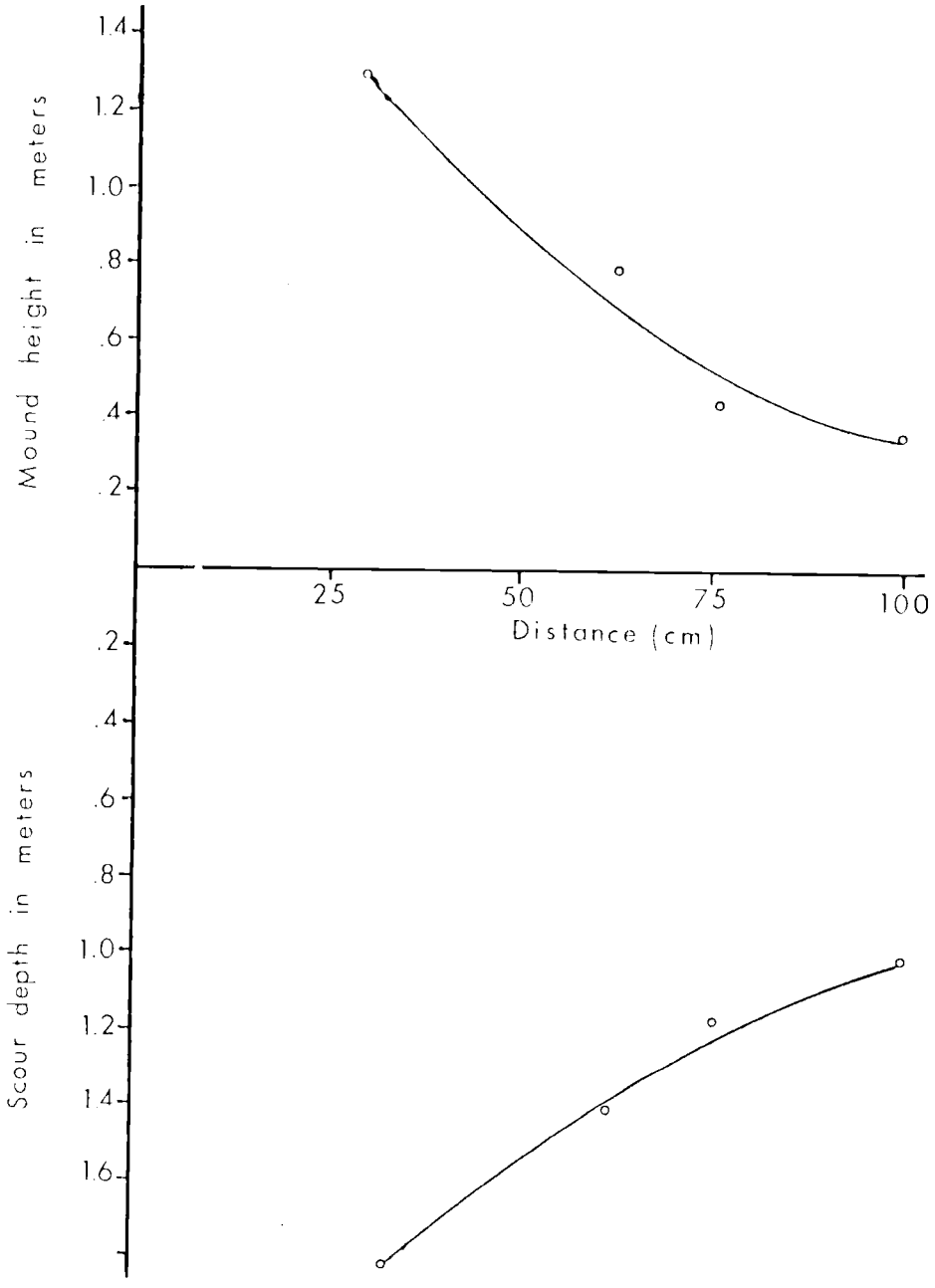


Figure 3. Scour depths and mound heights for changing distances between vessel's bottom and protective layer. (From Felkel and Steinweller, 1972)

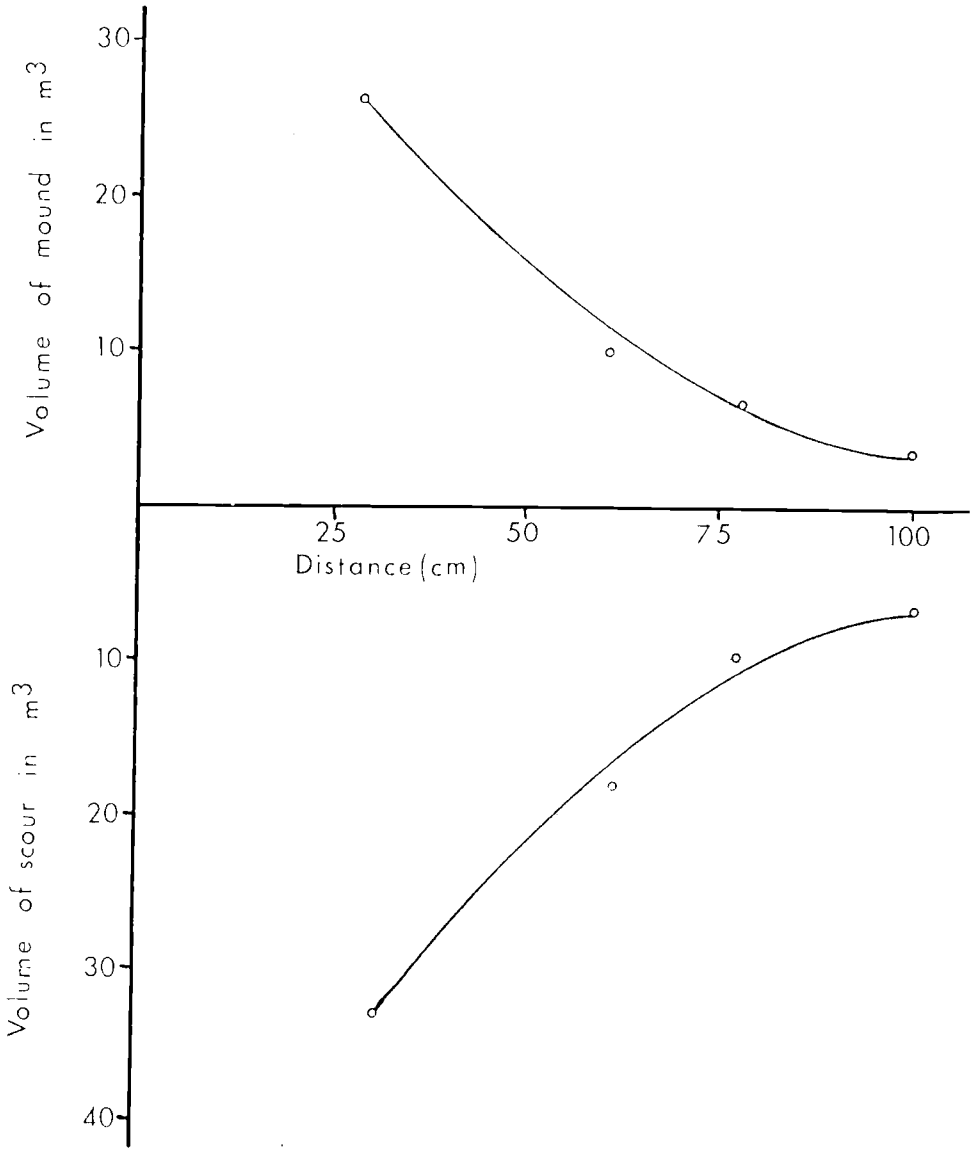


Figure 4. Volumes of scour and mound for changing distances between vessel's bottom and protective layer. (From Felkel and Steinweller, 1972)

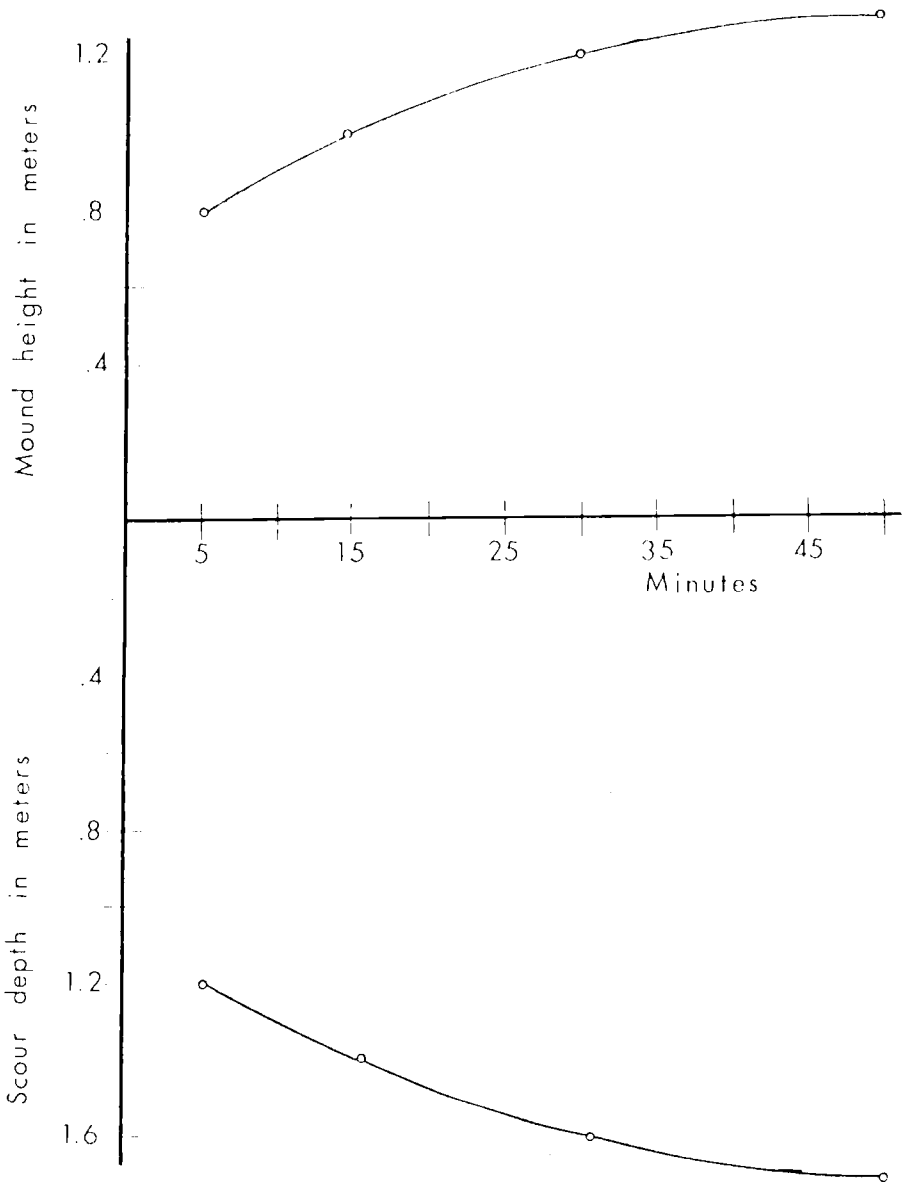


Figure 5. Chronological development of scour depths and mound heights with a 30 cm clearance between the bottom of vessel and protective layer. (From Felkel and Steinweller, 1972)

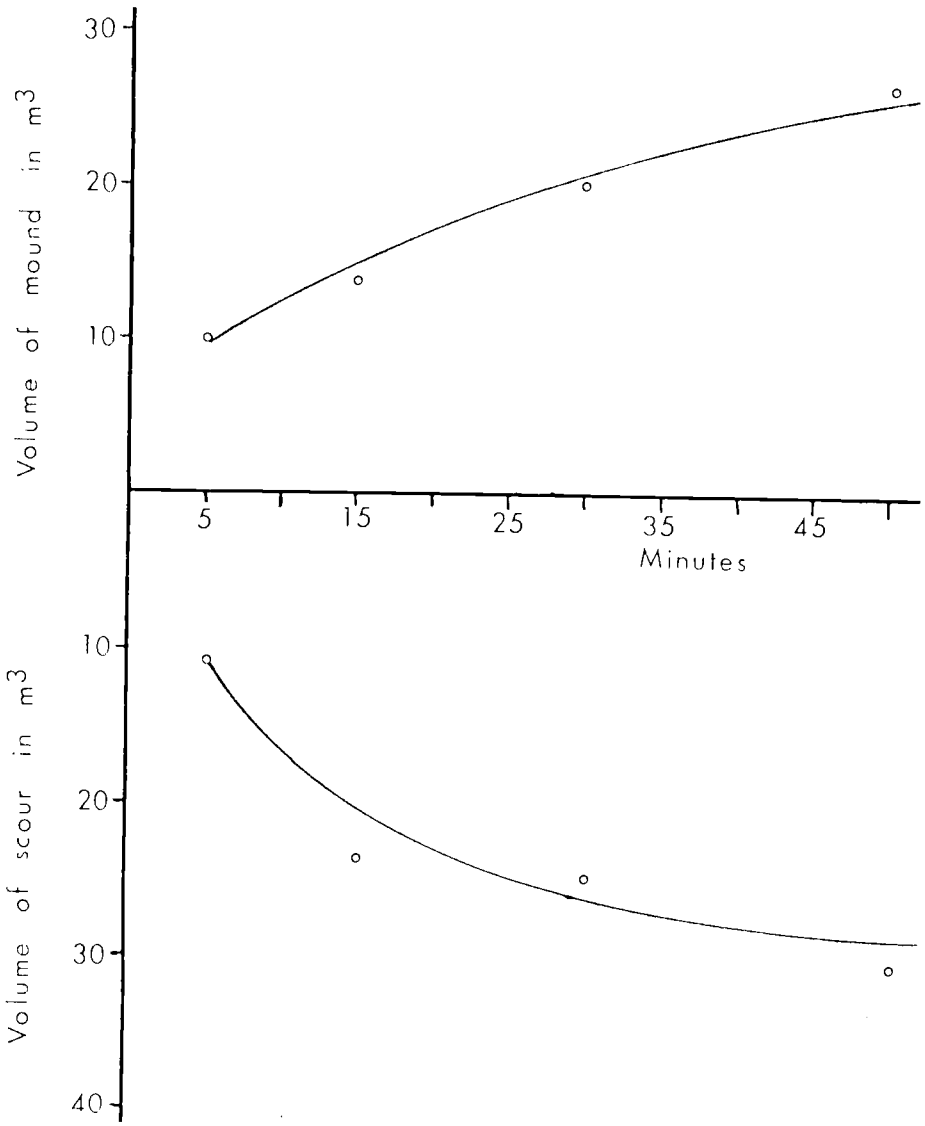


Figure 6. Chronological development of volumes of scour and mound in test with a 30 cm clearance between bottom of vessel and protective layer. (From Felkel and Steinweller, 1972)

in the Breisach Tests (Felkel and Steinweller, 1972). In these tests a ship with a draft of 1.56 meters, propeller diameter of 1.47 meters, and propeller rotational speed of 340 rpm's was used at two different water depths: 2.46 and 2.19 meters. Colored stones (weighing on the average 500 grams) were placed on the bottom to record the direction of bed movement caused by a ship passage. At the deeper water depth, no deformation of the bed was observed; only a few of the colored tracers having been moved underneath the vessel, usually a few decimeters in the ship's direction of travel. After the run at the shallower water depth, 2.19 meters, a groove 0.5 to 1.2 meters wide and 0.10 to 0.20 meters deep was noted. From all of the tests conducted, two conclusions were made regarding the movement of bottom material. In still water, most of the bed stones would be displaced in the direction of travel of a ship passing overhead. With a river current present, most of the stones would be displaced in the direction of river flow, regardless of whether the ship moved upstream or downstream. Therefore, in a river, the net sediment transport due to ship induced scour will always be downstream, while in a channel subjected to tidal currents, the sediment movement will be in the direction of the tidal currents.

To determine the extent of the propeller wake, an approximation of the wake can be obtained by separating it into two components: 1) an induced velocity caused by the shedding of vortices from the propeller and 2) an axial jet of water issuing from the propeller.

For the vortices that are shed by a propeller, the vortex intensity is proportional to the thrust (Slotta and Montes, 1975).

The vortex intensity,

$$\Gamma = \frac{2T}{\rho m \omega b^2} \qquad \text{(Breslin and Tsakona, 1959)} \qquad (2)$$

where $\rho$ is the density of water, m is the number of propeller blades, $\omega$ is the angular velocity of the propeller, b is the length of a propeller blade, and where the thrust, T, is defined as:

$$T = \frac{\rho A_0}{2} (U_0^2 - V_s^2) \qquad \text{(Streeter, 1966)} \qquad (3)$$

with $A_0$ being the circular area of a propeller disc, $U_0$ the velocity of water leaving the propeller, and $V_s$ the ship speed. If the vortices shed by a propeller are represented by a free vortex, the induced velocity can be given by:

$$v_\theta = \frac{\Gamma}{2\pi r} \qquad (4)$$

so

$$v_\theta = \frac{A_0 (U_0^2 - V_s^2)}{2m\omega r \pi b^2} \qquad (5)$$

where $v_\theta$ is the tangential velocity induced by the vortices and r is the radial distance from the propeller axis. Equation (5) shows that the tangential velocity component is inversely proportional to the distance from the propeller axis.

If the axial prop velocity is modeled as a jet of water in an infinite fluid the results obtained by previous investigators can be used to predict the decay of the axial velocity in the wake. It has been found that the decay of the centerline velocity in a water jet can be given by:

$$U_c/U_0 = 6.4\ D/x \qquad \text{(Harsha, 1971)} \qquad (6)$$

The decay of the lateral velocity distribution is shown in Figure 7, where

$$V/U_c = e^{-80(r/x)^2} \qquad \text{(Harsha, 1971)} \qquad (7)$$

Whereas the centerline velocity in a water jet is inversely proportional to the distance (Equation 6), the lateral velocity decays at a faster rate due to the exponential term (Equation 7). This indicates that the high velocity core exiting from the propeller does not extend very far in a lateral direction.

A more accurate representation of the propeller wake can be made by taking into account the free surface, because a jet of water near a free surface behaves differently than a jet in an infinite fluid. A shallow submerged axisymmetric jet has been found to deflect towards the free surface downstream of its nozzle. Initially the velocity profiles do not radically differ from those for an infinitely submerged jet. However, with increasing distance downstream, the velocities above the nozzle axis increase relative to those below the axis. As a consequence, the maximum velocity moves above the original nozzle axis and migrates upward with increasing distance downstream, eventually reaching the free surface (Maxwell and Pazwash, 1973).

Maxwell and Pazwash (1973) presented two mathematical models to describe a shallow submerged jet. For the near field region, $2.2 < x/D < 25$, it was found

$$\frac{\overline{V^2}}{(\overline{U^2})_0} = \alpha\left(\exp\left(\frac{-4\alpha}{D^2}\left(y^2 + (z-z_0)^2\right)\right) + \exp\left(\frac{-4\alpha}{D^2}\left(y^2 + (z+z_0)^2\right)\right)\right) \qquad (8)$$

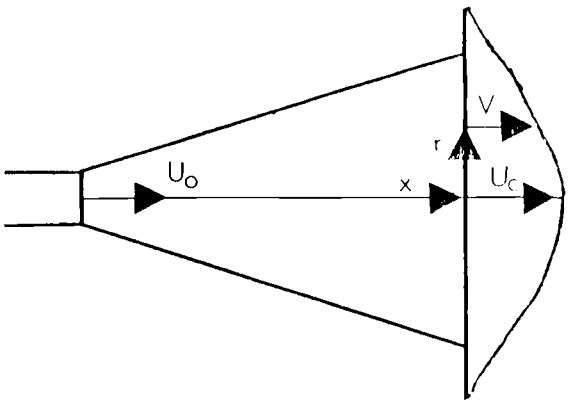


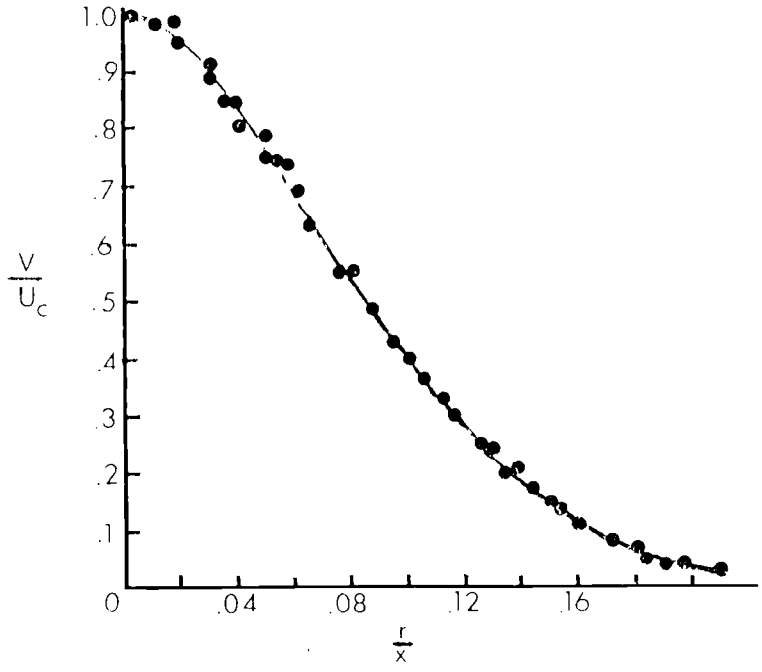


Figure 7. Lateral velocity distribution for an axisymmetric round jet. (From Harsha, 1971)

$$\text{where } \alpha = 1 - \exp(-D^2/4c^2x^2) \tag{9}$$

$c \simeq .083$, a constant spread coefficient, D is the diameter of the jet nozzle, $z_0$ is the location of the propeller axis below the surface and $\overline{V}/\overline{U}_0$ is the ratio of the mean velocity at a point to the mean velocity at the jet nozzle. At large distances from the jet nozzle, where $x/D > 25$, the submerged jet can be described by:

$$\frac{\overline{V^2}}{(\overline{U^2})_0} = \frac{D^2}{4c^2x^2} \left(\exp\left(-\frac{y^2 + (z_0-z)^2}{c^2x^2}\right) + \exp\left(-\frac{y^2 + (z_0+z)^2}{c^2x^2}\right)\right) \tag{10}$$

There are not enough data available in the literature to verify one model as being better than another. However, the jet described by Maxwell and Pazwash (1973) follows most closely the path of observed propeller wakes (Saunders, 1957), in that the effect of a submerged jet interacting with the surface is taken into account and the general flow in the propeller wake is toward the surface. Using the equations for a shallow submerged turbulent jet (Maxwell and Pazwash, 1973), the spread of a propeller wake for a typical ship in Coos Bay was calculated. Figure 8 shows the velocity ratio $\overline{V^2}/(\overline{U^2})_0$ plotted at various distances from the propeller at a depth corresponding to a channel bottom of 12.2 meters. Figure 8 shows that while there is a large spread in the jet, the high velocity core of the jet remains confined to a narrow region.

In conclusion, the high velocity core of a propeller wake does not always strike the bottom, but when it does, the wake might be expected to cause a considerable amount of scour. In many cases the propeller wake has decreased enough in magnitude when it reaches the

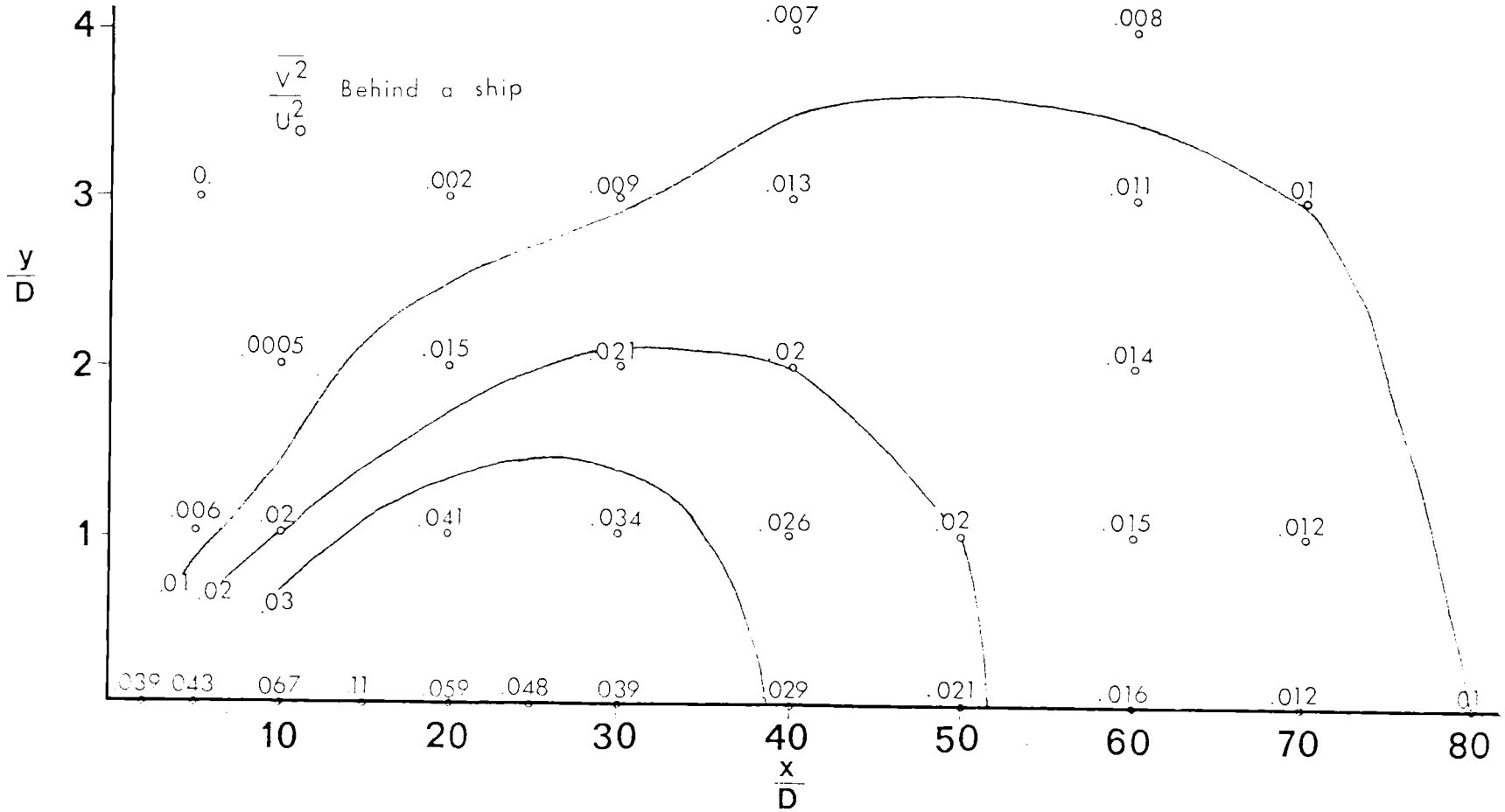


Figure 8. Spread of a propeller jet.

bottom so that it causes very little sediment movement. The velocity and size of a wake was found to depend on several variables: distance behind the ship, clearance beneath the ship, speed of the ship, and propeller rpm's.

# IV. FLOW AROUND A SHIP HULL

Even though the propeller wake might not extend to the bottom, it is still possible for scour to occur due to a ship's presence or its passage. When a ship moves through the water, it pushes water forward at the bow, displaces water alongside and underneath the hull, and drags water along behind the stern. These three currents are called respectively: the bow current, the return current, and the following current. The three currents are shown in Figure 9 for a typical velocity profile beneath a ship. These currents are of a sufficient magnitude that when a ship is operating in a narrow canal, the currents extend to the bottom and sides of the canal and can cause significant scour to occur in uncohesive soils.

## Bow Current

The bow current is formed by water being pushed ahead by a ship. The size of a bow current will therefore depend on the speed of the ship and the shape of its bow. A blunt bow, such as a barge, causes a larger bow current than a finely tapered ship. In the Kriegenbrunner Survey (1973), velocity profiles were made underneath two vessels at different water depths and ship speeds. Figures 10 and 11 show the current in proximity to the bottom beneath a ship and a barge. These figures show that the bow current is much smaller in size and magnitude than the return or following current.

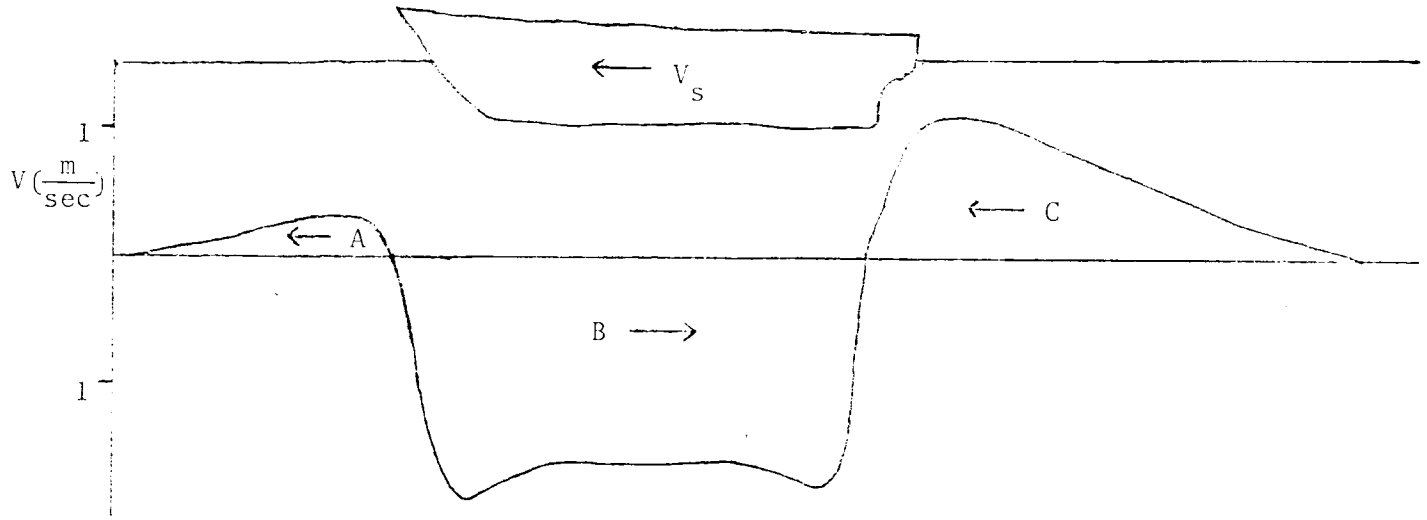


A - Bow Current
B - Return Current
C - Following Current

Figure 9. Typical velocity profile beneath a ship. (From Kriegenbrunner Survey, 1973)

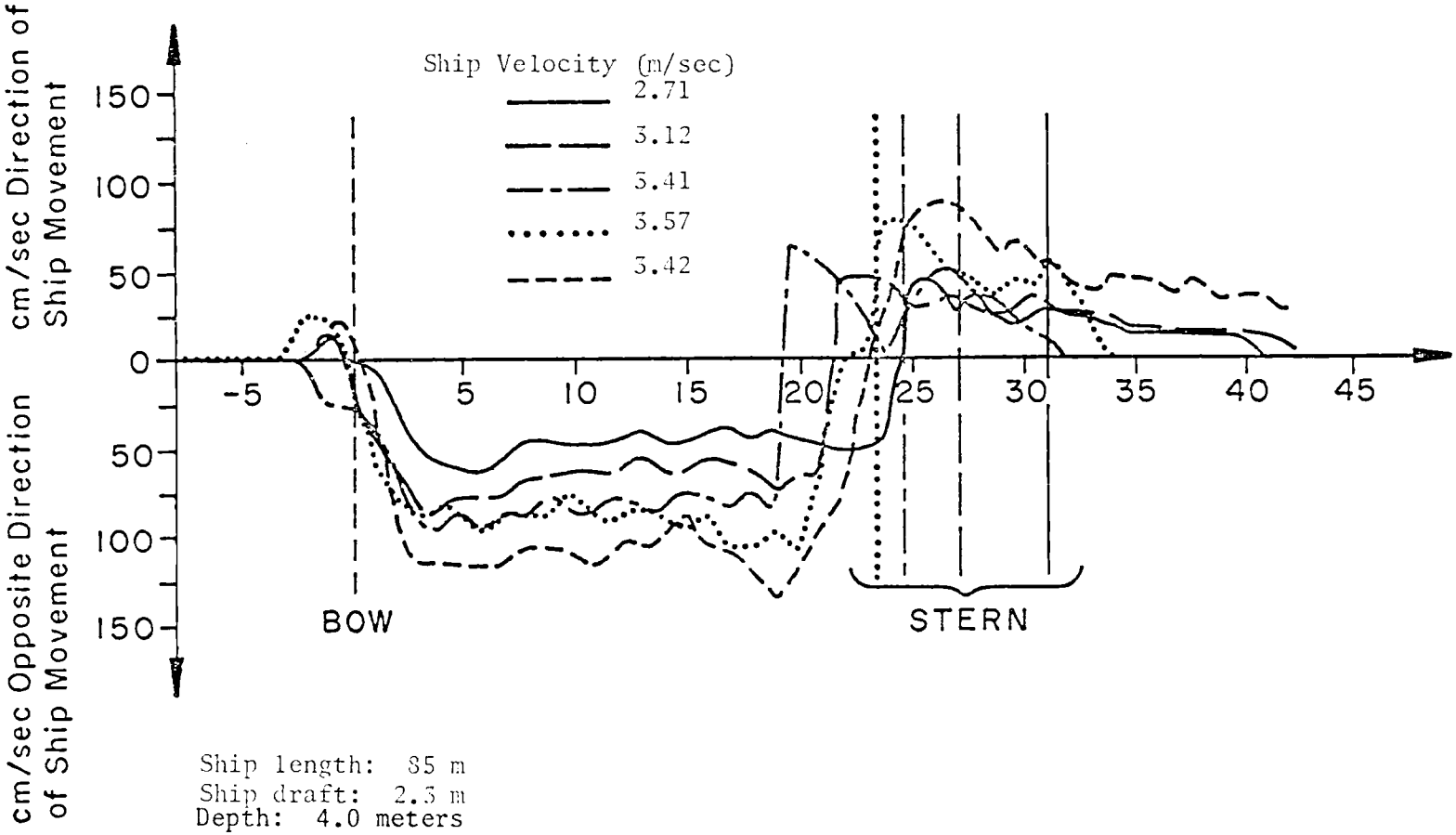


Figure 10. Current velocity near the bottom under a ship. (From Kriegenbrunner Survey, 1973)

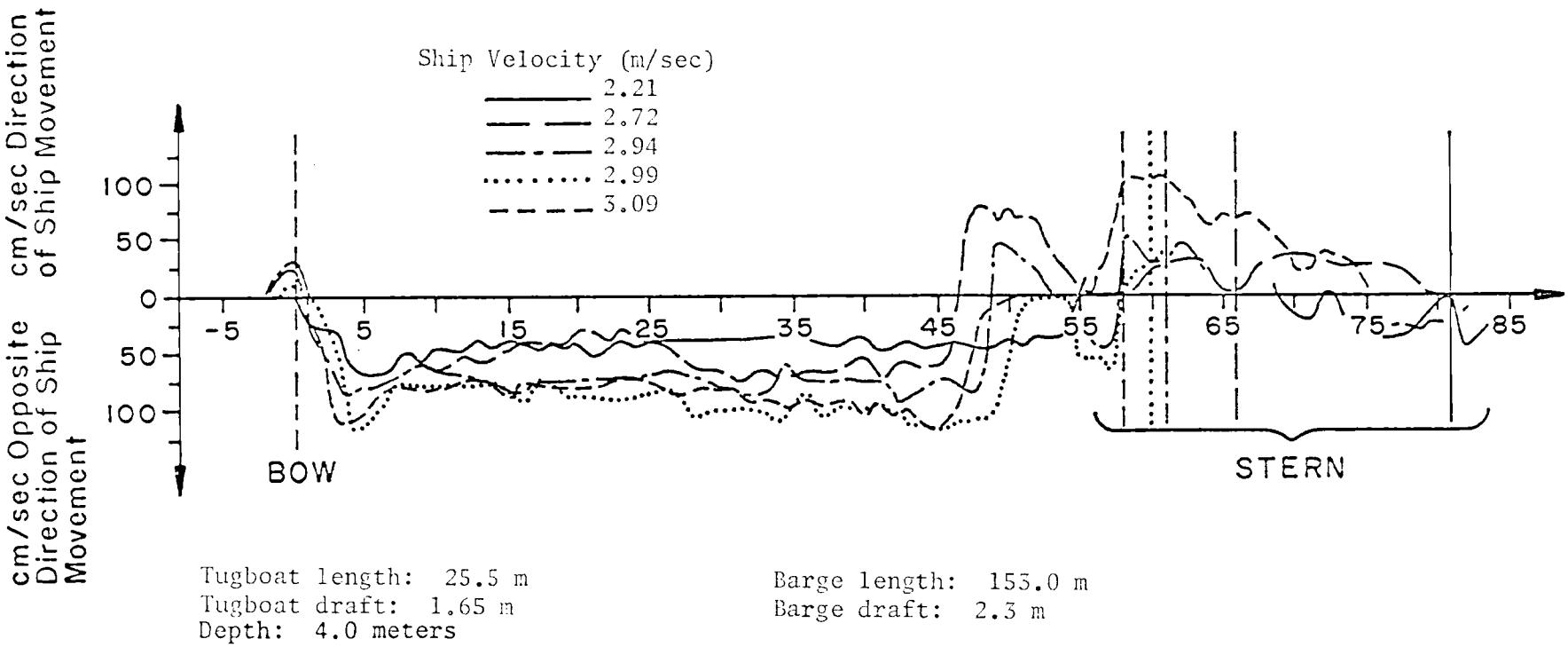


Figure 11. Current velocity near the bottom under a tug boat and barge. (From Kriegenbrunner Survey, 1973)

Return Current

The return current is caused by water flowing around and underneath a ship. The calculated streamlines in Figure 12 (Adee, 1973) show the proportion of water that flows underneath the ship as opposed to the amount that flows around the sides. Underneath a ship the return current reaches a maximum value just past the bow (Figure 9). From the tests in the 1973 Kriegenbrunner Survey, the investigators found the equation:

$$V_{r_m} = \frac{BD_1 V_s}{F_a - A} \tag{11}$$

to be a good predictor of the return current for ships in transit below their maximum possible speed in a canal; where $V_{r_m}$ is the mean velocity of the return current, B is the width of the ship, $D_1$ is the draft, $V_s$ is the ship speed, $F_a$ is the cross-sectional area of the canal, and A is the maximum cross-sectional area of the ship. This equation has not been verified in different canals, so its applicability for different size canals is not known. Past the bow the velocity decreases in magnitude and remains fairly constant until near the stern where a second maximum occurs before the return current ends and the following current begins.

The return current extends in a lateral direction for a considerable distance from a ship besides being present directly under the center of a vessel. Figure 13 shows the velocity measured .88 meters above the canal bottom at three distances from a ship. Figure 13 gives a satisfactory representation of the general shape of the longitudinal

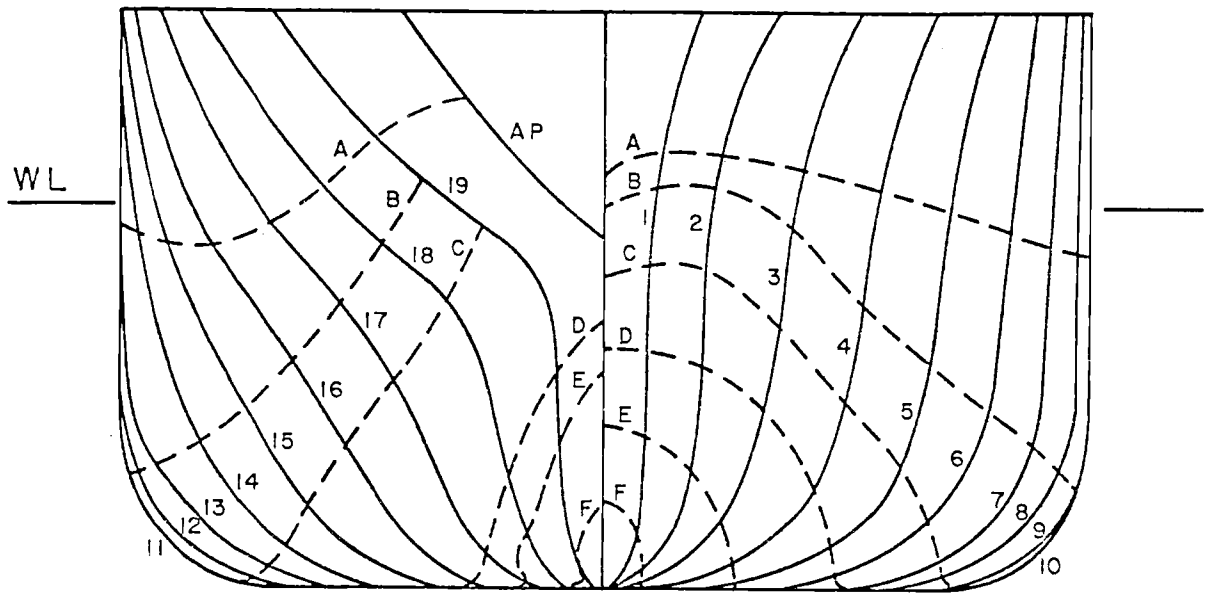


Figure 12a. Calculated streamlines about a Series 60 ship. (From Adee, 1973)

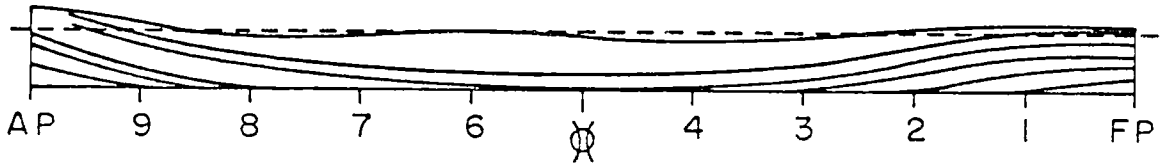


Figure 12b. Centerplane projection of the streamlines about a Series 60 ship. (From Adee, 1973)

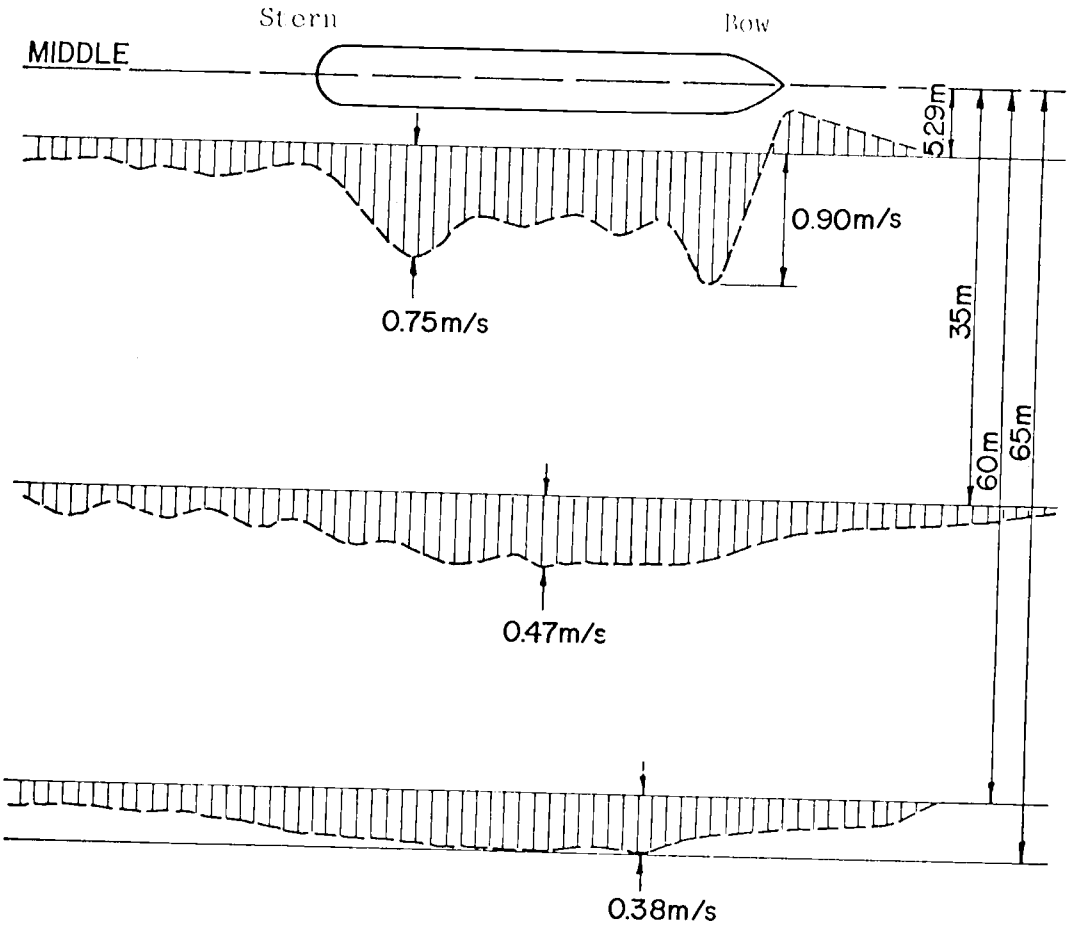


Ship: Adriaan
Place: Middle of Canal
Draft: 2.58 meters
Water depth: 6.0 meters
Beam: 9.5 meters
Length: 80 meters
Ship speed: 4.83 meters/second
Scale: 1 cm = .40 meters/second
Velocity measured .88 m above the bottom.

Figure 13. Longitudinal velocity profiles in a lateral direction from a ship. (From Delft, 1974)

velocity profile in the lateral direction. However, the specific velocity profile for any ship will depend on the type and speed of the ship and the canal dimensions. Figures 14 and 15 illustrate that the current velocity changes with a change in ship speed and draft. Note, for these figures there was only a small change in the draft between the two tests, there was accordingly little difference in the return current velocities, the range in propeller rpm's though, was large enough to show that the return current depends strongly on the rotational speed of the propeller.

The size of a canal and the location of a ship in the canal also affects the flow around a ship. Figures 16a, 16b, and 16c show velocity contours near the canal bottom and surface for one ship in three different canals. Figure 16a shows a larger current velocity than was present in the other canals due to a smaller canal cross-sectional area. The same narrowing effect occurs when a ship moves from the canal centerline towards one bank. The decrease in area between the ship and the bank causes an increase in the current velocity. The velocity profile presented in Figure 15 was made at the edge of a canal while a barge passed in the middle of the canal; whereas Figure 17 presents the velocity profile taken at the same location but with the barge 23.6 meters closer to the canal bank. Significant velocity differences can be discerned by comparing these two figures. Both the canal cross-sectional area and the ship speed are the major factors influencing the return current.

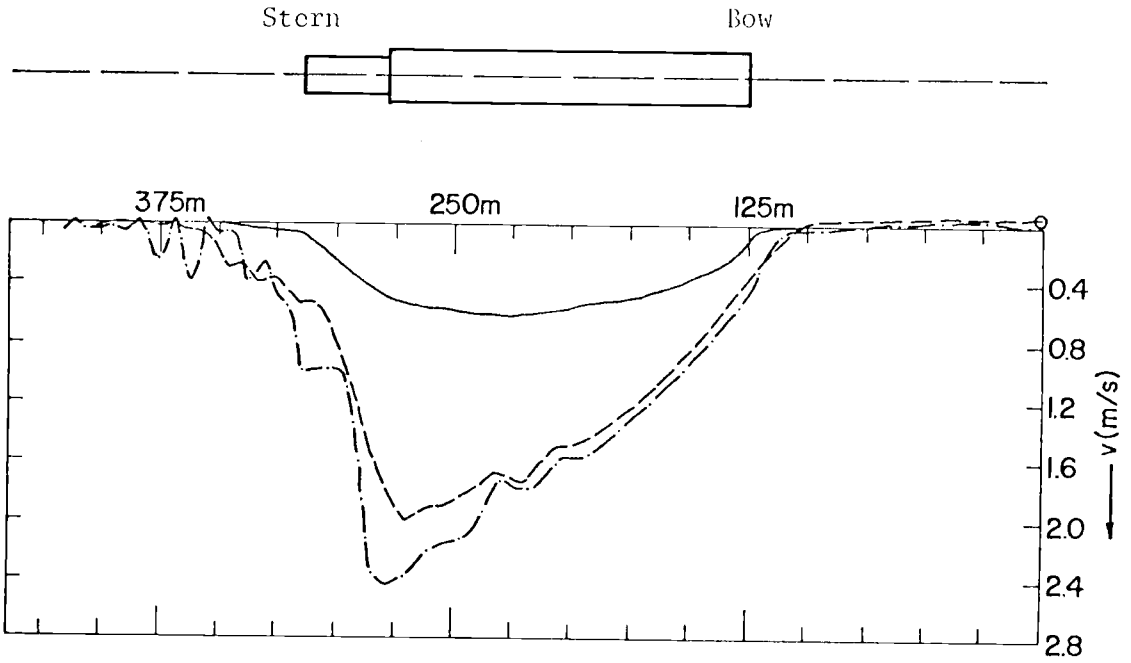


Canal bottom width: 120 m
Ship: Tugboat + 4 barges
Location of Ship: Middle
Draft: 3.30 meters
Velocity measured at edge of slope, 1 m above the bottom.
Water depth: 6 meters

———— 1000 rev/min. Ship speed: 3.71 meters/second
— — — — 1600 rev/min. Ship speed: 4.57 meters/second
—.—.—.— 1800 rev/min. Ship speed: 4.53 meters/second

Figure 14. Current velocity at the edge of the Scheldt-Rhine canal, ship draft of 3.3 m. (From Delft, 1974)

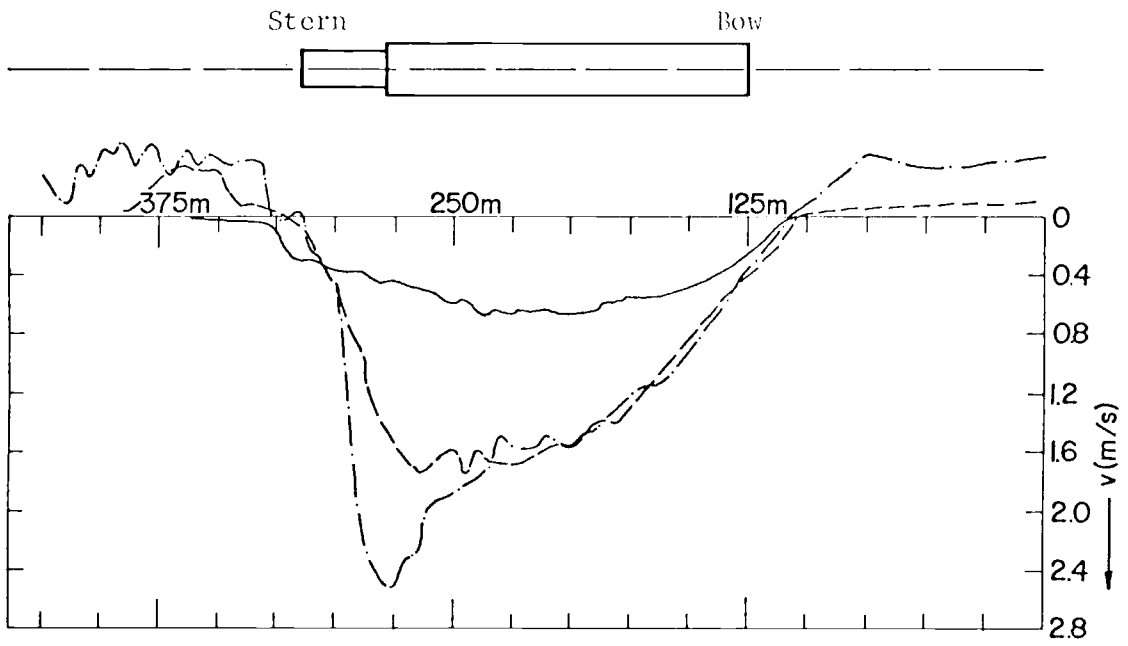


Canal bottom width: 120 m
Ship: Tugboat + 4 barges
Location of ship: Middle
Draft: 4 meters
Velocity measured at edge of slope, 1 m above the botton.
Water depth: 6 meters
———— 1000 rev/min. Ship speed: 3.22 meters/second
— — — — 1600 rev/min. Ship speed: 4.26 meters/second
—.—.—.— 1800 rev/min. Ship speed: 4.24 meters/second

Figure 15. Current velocity at the edge of the Scheldt-Rhine canal, ship draft of 4 m. (From Delft, 1974)

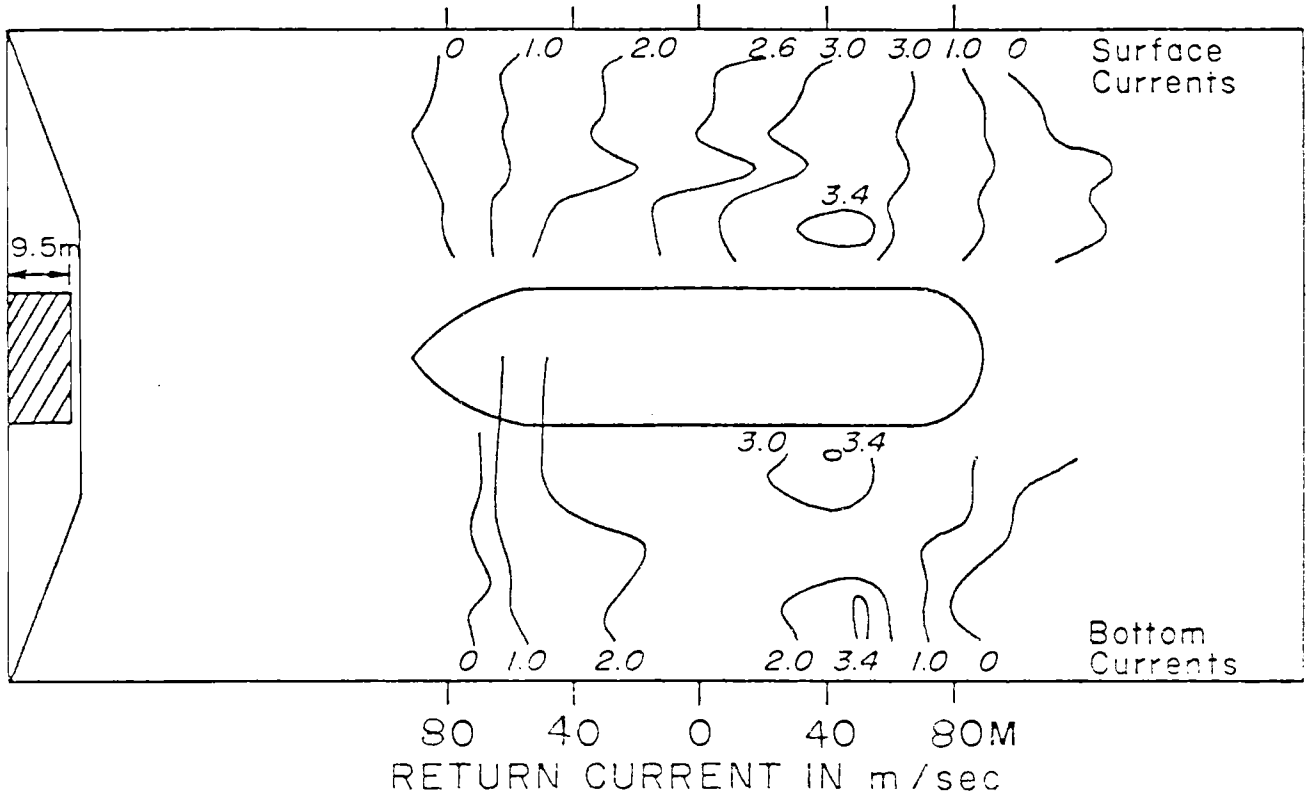


Figure 16a. Surface and bottom return currents around a ship in three different canals. (From Wasser-und Schiffahrtsdirektion Kiel, 1966)
a. n = 4.18 $V_s$ = 14 km/hr Canal bottom width: 44 m

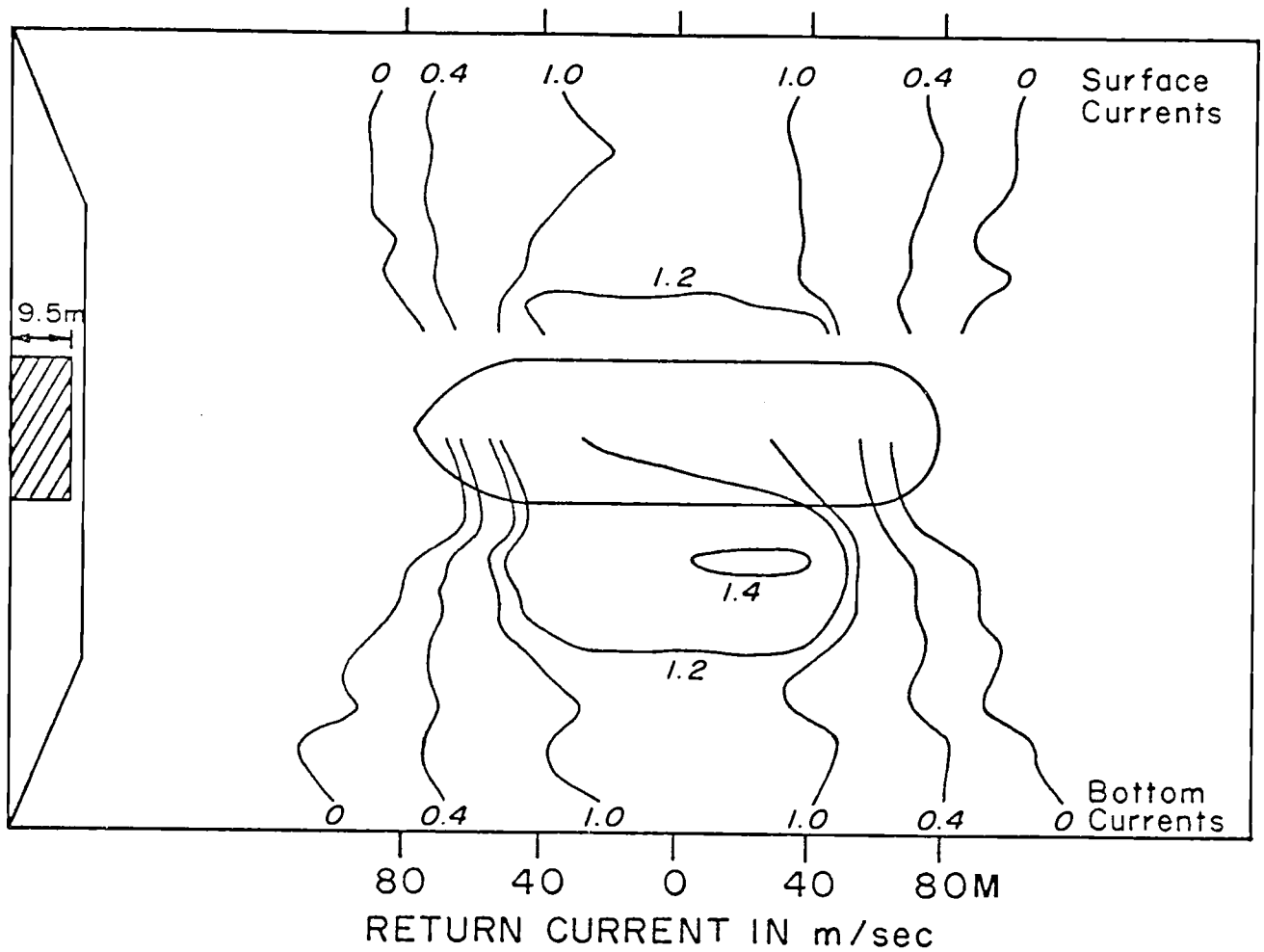


Figure 16b. Surface and bottom return currents around a ship in three different canals. (From Wasser-und Schiffahrtsdirektion Kiel, 1966)
b. n = 5.8 $V_s$ = 14.5 km/hr Canal bottom width: 72 m

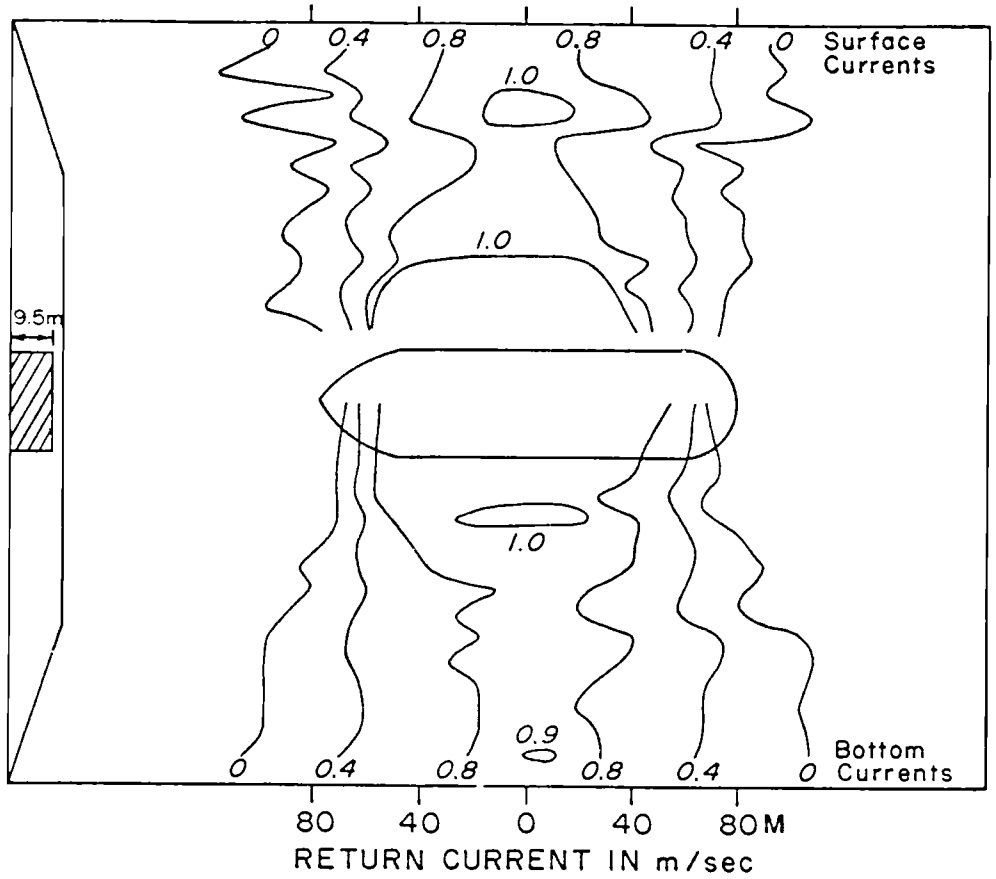


Figure 16c. Surface and bottom return currents around a ship in three different canals. (From Wasser-und Schiffahrtsdirektion Kiel , 1966)
c. n = 7.1 $V_s$ = 14.5 km/hr Canal bottom width: 95 m

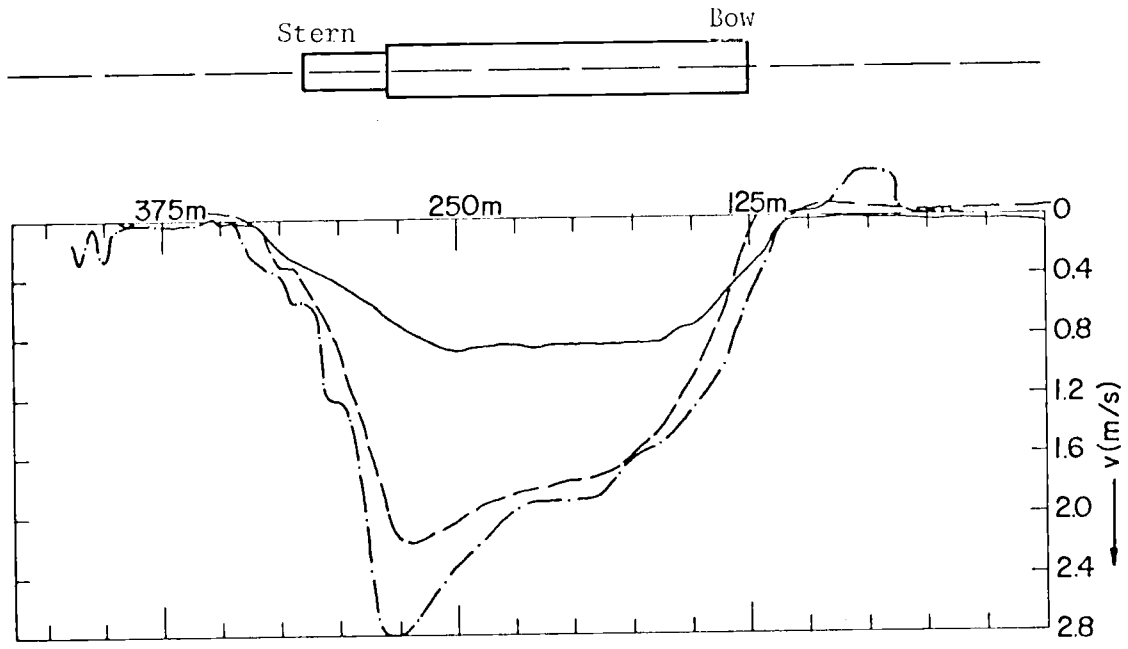


Canal bottom width: 120 m
Ship: Tugboat + 4 barges
Location of ship: 23.6 m from the middle
Draft: 4 meters
Velocity measured at edge of slope, 1 m above the bottom.
Water depth: 6 meters

———— 1000 rev/min. Ship speed: 3.20 meters/second
— — — — 1600 rev/min. Ship speed: 4.21 meters/second
—·—·— 1800 rev/min. Ship speed: 4.23 meters/second

Figure 17. Current velocity at the edge of the Scheldt-Rhine canal, ship draft of 4 m, ship 23.6 m from the canal centerline. (From Delft, 1974)

## Following Current

The following current is formed by water flowing in behind a ship and traveling along with the ship. Figure 9 shows that the following current reaches a peak near the stern and then decays to zero. In the 1973 Kriegenbrunner Survey, the maximum value of the following current beneath a ship was found to be approximately equal to the maximum value of the return current under the ship. In the Delft studies, Figures 14, 15 and 17, it can be seen that the following current does not extend as far in the lateral direction as the return current. Figure 18 shows the extent of the following current along with the bow and return current for a tugboat pushing a barge.

## Mathematical Model

If a method could be obtained for estimating the velocity distribution around a ship, then it would be helpful to predict in advance what ship speeds would produce associated current velocities high enough to cause scour in canals of specified dimensions and materials. A number of investigators (Denny, 1963; Hess and Smith, 1964; Plotkin, 1975, 1976; Tuck, 1966; Tuck and Taylor, 1970) have presented analytical developments concerning flows around hull shaped objects. The works by Plotkin (1975) and Tuck (1966) were found to be the most applicable to the present problem in considering ship movements in shallow water.

Plotkin (1975) and Tuck (1966) used the method of matched asymptotic expansions to analyze the potential flow field of a slender ship moving in shallow water. Shallow-water theory describes the flow in

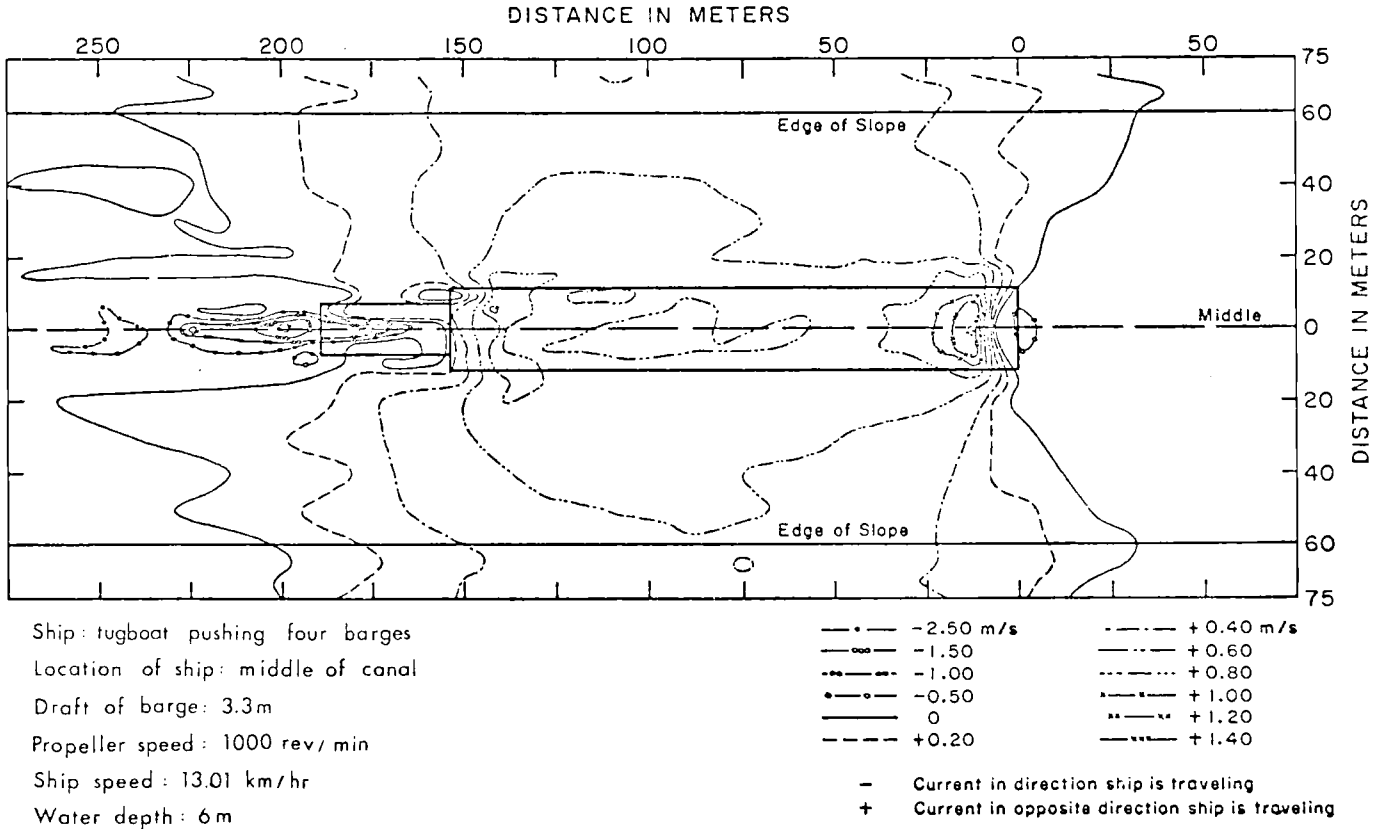


Figure 18. Current velocity contours around a tug boat and barge in the Scheldt-Rhine canal. (From Delft, 1974)

the far field and slender body theory provides the near-field description. Plotkin and Tuck used the results of the potential flow solution to calculate the forces on a ship hull, but the same results can similarily be used to describe the velocity field near a ship hull.

The following is a formulation of the problem of flow past a slender ship in shallow water (Plotkin, 1975 and Tuck, 1966). Consider the steady subcritical potential flow of a stream of shallow water of speed U past a slender ship of length 2L. The coordinate system is shown in Figure 19. x lies in the stream direction and z is measured upwards from the undisturbed free surface. The fluid is taken to be inviscid and incompressible and the flow is steady. A disturbance potential, $\phi$, exists which satisfies Laplace's equation and tends to zero at infinity. The total fluid velocity, $\vec{q}$, is given by:

$$\vec{q} = U\nabla (x+\phi) \tag{12}$$

where $\nabla$ is the differential operator.

The slenderness assumption requires the beam and draft to be small compared to the length, say of $O(\varepsilon)$. The hull is described by the equation:

$$y = \varepsilon f(x,z) \tag{13}$$

The kinematic boundary condition on the ship surface for this inviscid flow requires that the body be a flow streamline, so that

$$\phi_y - \varepsilon(1+\phi_x)f_x - \varepsilon\phi_z f_z = 0 \text{ on } y = \varepsilon f \tag{14}$$

The shallowness assumption also requires the depth to be $O(\varepsilon)$. On the

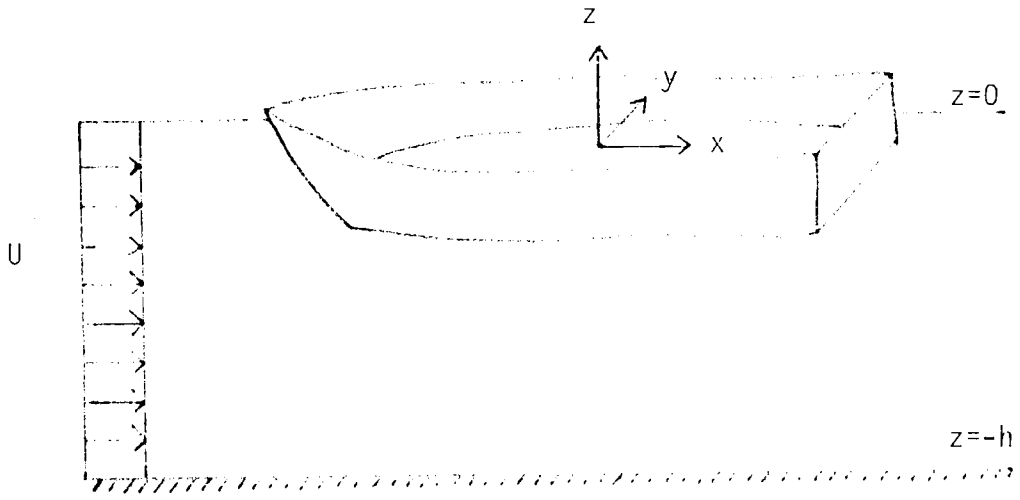


Figure 19. Coordinate system and flow schematic for potential flow problem.

bottom, assumed to be a plane surface at $z = -\varepsilon h_0$, we have

$$\partial\phi/\partial z = 0 \quad \text{on } z = -\varepsilon h_0 \tag{15}$$

The boundary conditions on the unknown free surface

$$z = \eta(x,y) \tag{16}$$

are firstly that the pressure vanishes

$$-2g\eta/U^2 = 2\phi_x + \phi_x{}^2 + \phi_y{}^2 + \phi_z{}^2 \tag{17}$$

and secondly that the free surface is a streamline

$$\phi_z = \eta_x + \phi_x\eta_x + \phi_y\eta_y \tag{18}$$

The depth Froude number

$$F^2 = U^2/g\varepsilon h_0 \tag{19}$$

is taken to be of 0(1).

The procedure for solving this problem can be found in papers by Plotkin (1975, 1976) and Tuck (1966), therefore only the results will be presented here. The velocity component in the x direction is given by:

$$u = U(1+\phi_x) \tag{20}$$

Since only the increase in velocity over the free stream velocity is of concern, the velocity to be determined is:

$$u = U\phi_x \tag{21}$$

From Plotkin (1975)

$$\phi_x = -\frac{1}{2}\,\frac{\varepsilon}{\pi h_0(1-F^2)}\,\frac{1}{2}\int_{-\infty}^{\infty} d\xi\,\frac{S_a'(\xi)}{x-\xi} \tag{22}$$

For an ellipsoidal hull of revolution described by:

$$x^2/L^2 + y^2/B_0^2 + z^2/B_0^2 = 1 \tag{23}$$

the area $S_a(x)$ is given by:

$$S_a = 0.5\pi B_0^2(1-x^2/L^2) \tag{24}$$

Using Equations 22 and 24, the velocity along the hull can be described by:

$$u = U\left(-\frac{1}{2}\,\frac{B_0^2\varepsilon}{h_0 L(1-F^2)^{\frac{1}{2}}}\left(\frac{x}{L}\,\mathrm{Ln}\left|\frac{1+x/L}{1-x/L}\right| - 2\right)\right) \tag{25}$$

To see how accurate this representation of the velocity is in describing the velocity beneath a ship, the velocities measured in one test of the Kriegenbrunner Survey (1973) were compared to the predicted velocities for a hull of revolution with a parabolic waterline that had the same length and draft as the ship in the test. Figure 20 shows the calculated and measured velocities beneath the ship. From Figure 20 it can be seen that Plotkin's model is not very accurate in predicting the velocity under a ship and additional analytical work needs to be done in this area in order to accurately predict the flow field around a ship.

A paper by Beck, Newman, and Tuck (1975), which appears to offer an improvement over Plotkin's model, arrived too late for inclosure in

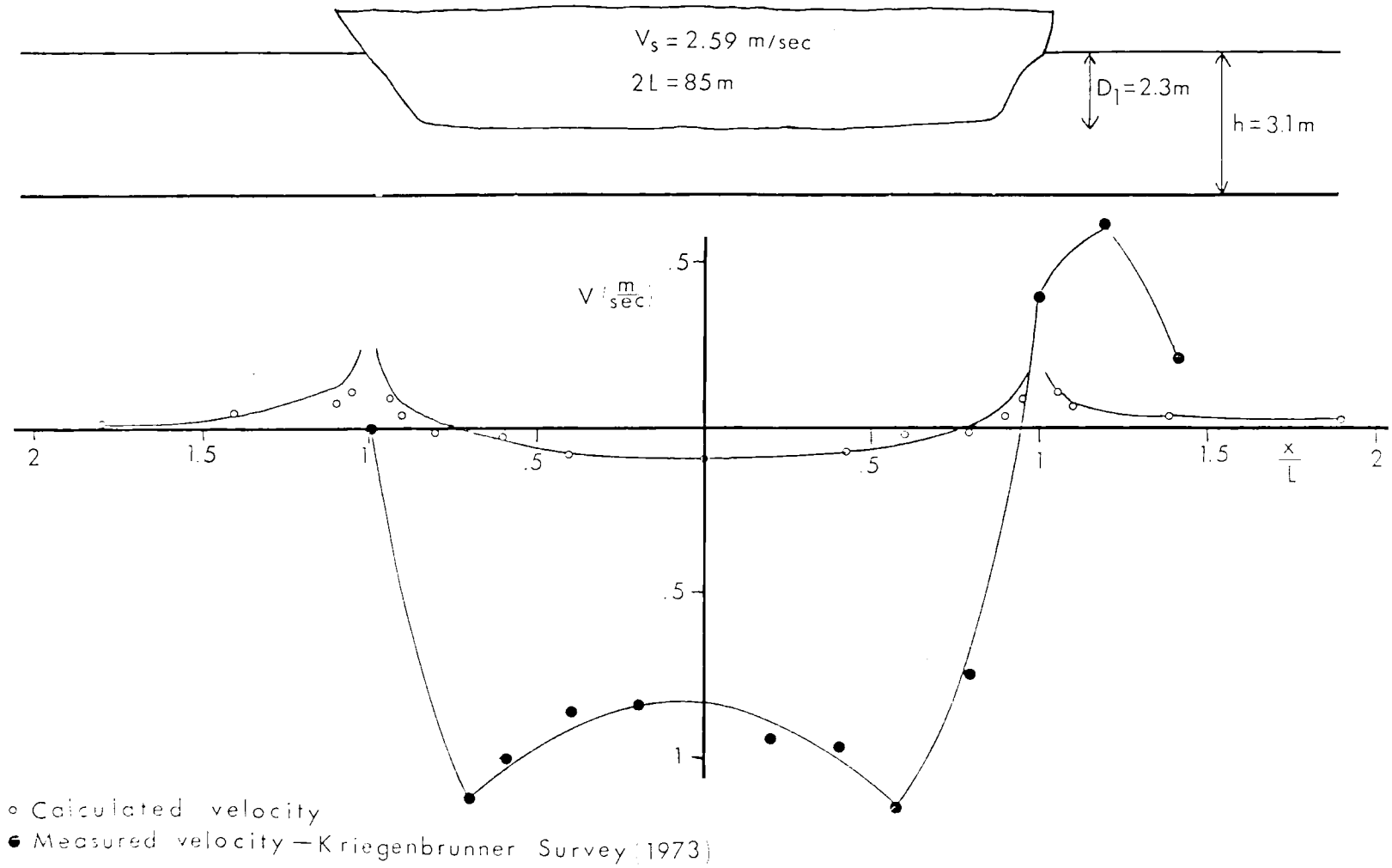


Figure 20. Comparison of calculated velocity with measured velocity beneath a ship.

this report. In the paper, entitled "Hydrodynamic Forces on Ships in Dredged Channels," a velocity potential is presented for flow around a ship in a canal with a finite depth and width and surrounded on both sides by shallow water. Beck, Newman, and Tuck looked at the sinkage, trim, and wave resistance of a ship, but their results can be extended to describe a velocity field around a ship.

# V. SHIP WAVES

## Formation of Waves

When a ship moves forward, water is deflected around the hull and a dynamic pressure distribution develops over the hull surface in contact with the water. The dynamic pressure is positive and generally maximum at the bow, dropping to a negative value over most of the midsection and becoming positive again near the stern. The positive and negative dynamic pressures cause the water's free surface to respond by rising and falling as a vessel moves through the water creating surface water waves. In the ocean the waves mix with wind waves and swell or decay with distance. However, in harbors the waves cannot decay over a large distance, so the canal banks must absorb the energy in the waves.

The energy contained per unit of wave surface is directly proportional to the square of the wave height,

$$E/\ell\lambda = \gamma H^2/8 \tag{26}$$

where E is the energy, $\ell$ is the crest length, H is the wave height, $\lambda$ is the wave length, and $\gamma$ is the specific weight of water. Thus, wave height is of principal interest in considering the effect a wave has on river banks. Sorensen (1967b) found that the heights of waves generated by a ship are almost entirely dependent on the ship's speed. Faster moving ships created larger waves than slow ships. Das and Johnson (1970) found that the wave height decreases with distance in the wake of a ship. However, in a confined waterway, the banks are

close enough to shipping lanes to prevent a significant amount of wave decay.

Erosion from Waves

Waves propagating into shallow water can cause erosion in any one of three ways. When a wave is in deep water, the orbital velocity of the wave does not reach the bottom. As a wave moves into shallow water, the orbital velocity presence is felt at the bottom. A small increase in water velocity at the bottom will initially cause a mixing of the water column that will cause a decrease in the sediment concentration. As the wave moves into more shallow water, the bottom velocity increases and sediment resuspension takes place. Anderson (1974) found that a velocity between 10 and 20 cm/sec was large enough to cause either a mixing of the water column or a resuspension of the fine-grained estuarine sediments.

Ship waves mainly erode the canal banks near the water level, where waves break. As a wave travels into shallow water, the wave celerity decreases and the wave crest steepens until the wave eventually breaks. The impact of a breaking wave causes a resuspension of the fine material along the shoreline. Even if the waves do not break, they can still cause damage to the banks. The rapid fluctuations of the waver level caused by even small waves can cause pressure gradients in the subsoil that can result in the uplifting of parts of the bank and resulting in the washing-out of particles from the subsoil. The alternate motion of runup and backwash of the waves on the shore causes erosion until an equilibrium slope is reached. Steep or

near vertical river banks will continually be attacked by waves, and if the bank material is erodible or unstable, bank failure can be expected.

Waves in Coos Bay

In many areas of Coos Bay the banks at the shore are vertical, but the only time they are exposed to waves is at high tide. At other times the waves runup on tidal flats. The ship induced waves at Coos Bay have been found to be either very small or nonexistent. This is due to the slow speed at which the ships operate in the channel. Conversations with Coos Bay pilots, Mr. Hansen and Mr. Davis (Oct. 1975), revealed that cargo ships operate at speeds from 1.0 - 1.5 m/sec in the upper part of the harbor and from 4.1 - 4.6 m/sec in the lower part of the harbor.

While cargo ships do not usually create waves in the harbor, tugboats do create waves. The size of such waves are found to depend on the speed and size of the craft. The maximum height of the tugboat waves observed in Coos Bay has been 0.3 meters. With a wave of 0.3 meters, the maximum horizontal particle velocity at the sediment-water interface can be obtained by:

$$U_{max_{bottom}} = \frac{H(g(H+h))^{\frac{1}{2}}}{2h} \quad \text{(Anderson, 1974)} \qquad (27)$$

where H = wave height and h = water depth. With a wave height of 0.3 meters and a water depth of 0.61 meters, the maximum horizontal velocity would be 0.76 m/sec. The velocity from the tug waves is less than the maximum tidal current velocity, 1.04 to 1.8 m/sec (Coos Bay

EIS Supplement, 1975). This indicates that while the tugboat waves might cause mixing and resuspension of some bottom sediments, the tidal and river currents have a larger potential for eroding bottom materials.

In determining the effect ship waves have on sediment resuspension, it has been related that the most important characteristic of the wave is its height which is known to depend mainly on the ship's speed. In Coos Bay, Oregon, cargo ship's speeds are low enough so that waves of negligible height are produced. Even though tugboats have been observed to produce waves, it can be said that river and tidal currents cause more sediment resuspension than ship's waves.

# VI. SHIP INDUCED EROSION

The erosion in a canal can not be easily separated into the proportions caused by the propeller wake, or flow around a ship hull, or that caused by a ship's waves. All three processes are interrelated and contribute to the erosion under different circumstances. The erosion that does occur can be arranged in two categories: bed load transport and sediment resuspension. While describing the bed load transport and sediment resuspension does not give an indication of the total quantity of sediment scoured, it does provide an individual with a clear picture of the erosion process. Bed load transport was discussed in a previous section and sediment resuspension will be covered next.

## Sediment Resuspension

Sediment resuspension caused by ships is known to exist (Anderson 1974, Hart 1969, and Karaki, et al. 1975). Whether the resuspension is detrimental to the water quality of the area depends on many factors. One of the most important considerations is the background turbidity level in the channel. Turbidity is a measure of the scattering of light as it passes through water. It is caused by the presence of suspended material in the water and is measured in terms of one milligram of silicon dioxide dissolved in a liter of water (Jackson Turbidity Unit or JTU).

How harmful the turbidity increase caused by a ship passage is depends on the background turbidity level. If the background level is

already high, the passage of a ship might not have any noticeable effect on the turbidity. Karaki and van Hoften (1975) described a very simple relationship which assumes that the turbidity at a point in the river increases as a ship passes (Figure 21a). The turbidity in the river rises to a maximum value behind the ship and then decays to the background level. When another ship approaches before the turbidity level has returned to normal, the effect of the two ships is cumulative (Figure 21b). For a low background turbidity level, this would be a significant increase in turbidity. While for a high background level, the added turbidity might be barely discernable. The model presented by Karaki and van Hoften was not substantiated by any field data, but was meant to represent qualitatively the change in the turbidity level.

The deposition location of the suspended sediments depends on the particles settling velocity and the river current. The settling time varies depending on the size of the particle and the stream turbulence levels present in the water. The average settling velocity of a particle in turbulent water can be considerably reduced below its terminal settling velocity in still water. For quartz grains, Murray (1970) predicts a reduction in the settling velocity on the order of 30%. The longer a particle remains in the water column, the farther it will be transported before it is deposited.

Estimate of Erosion in a Canal

Instead of looking at the different forms of erosion, it is more useful to look at what overall parameters are important in determining

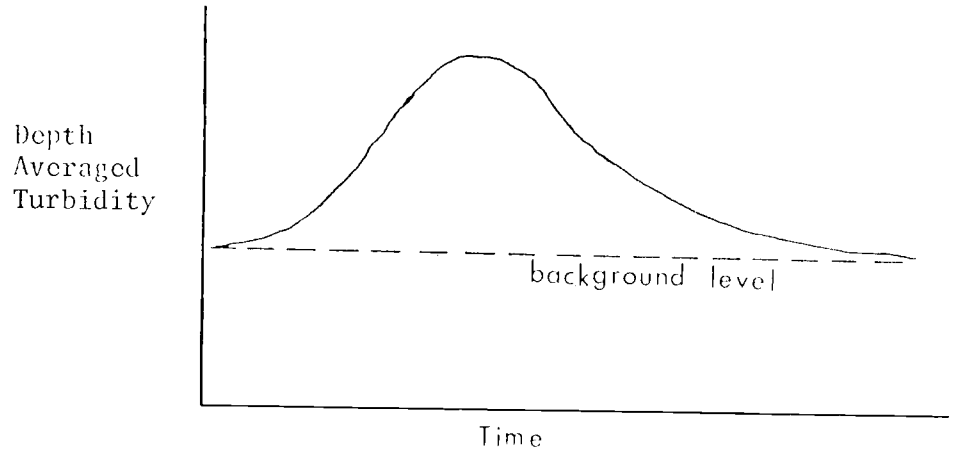


a. Turbidity increase after the passage of one ship.

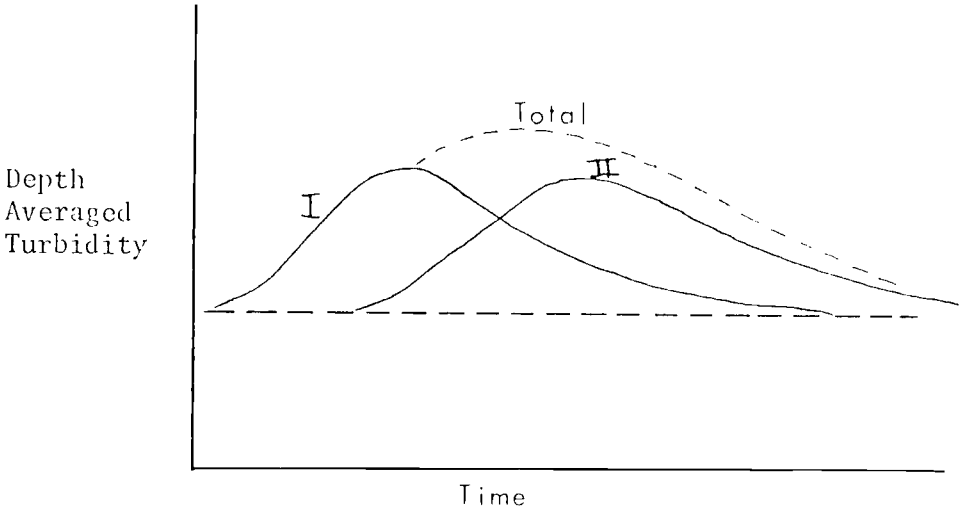


b. Two ships passing in succession.

Figure 21. Effect of ship traffic on stream turbidity. (From Karaki and van Hoften, 1975)

the scour in a canal caused by the passage of a ship. In tests concerning the Kiel Canal conducted by SOGREAH (Wasser und Schiffahrtsdirektion Kiel, 1966), it was found that n, the ratio of canal cross-sectional area to maximum ship cross-sectional area, and the ship speed were the two most important parameters in determining the amount of erosion that would take place in a canal.

The SOGREAH tests were conducted with three different size ship models representing the main classes of ships that use the canals being studied. The normal operating speed for the ships is from 8.0-19 km/hr, with the smaller ships generally traveling at the faster speeds. Characteristics of the different ships are listed in Table II.

TABLE II. CHARACTERISTICS OF SHIPS IN SOGREAH TESTS

| Class | Displacement Tons | DWT | Draft m | Length m | Cross-Sectional Area $m^2$ |
|---|---|---|---|---|---|
| 1 | 26000 | 12500 | 9.5 | 155 | 198.0 |
| 2 | 16000 | 8000 | 8.5 | 125 | 165.6 |
| 3 | 10000 | 5000 | 7.5 | 105 | 126.0 |

The canals used in the tests were modeled after existing and proposed waterways. Five different size canals were used, which provided a range in the cross-sectional area from 828 $m^2$ to 1408 $m^2$. With the size of the ships tested, this provided a range in n from 4.2 to 11.2. The sediment in the canals consisted of two different types of sand. One type of sand had a density of 2.68 $gm/cm^3$ with $D_{50}$ = .2mm, while the other type of sand had a density of 2.66 $gm/cm^3$ with $D_{50}$ = .7mm. The erosion that took place in each canal was determined by the

deposition of material on the bottom of the canal. From the deposited material, an estimate could be made of the volume of sand ($m^3$) eroded per meter of canal length ($m^3/m$ ) for 100 ship passages.

The results of the SOGREAH tests are summarized in Figure 22, which shows the erosion rate versus the ship Froude number for different values of n. Data in Figure 22 give an indication that the erosion rate increases when the speed of a ship increases or when n decreases. From Figure 22, it is possible to determine the amount of erosion that occurs due to each class of ship and accordingly find the total expected erosion in a canal.

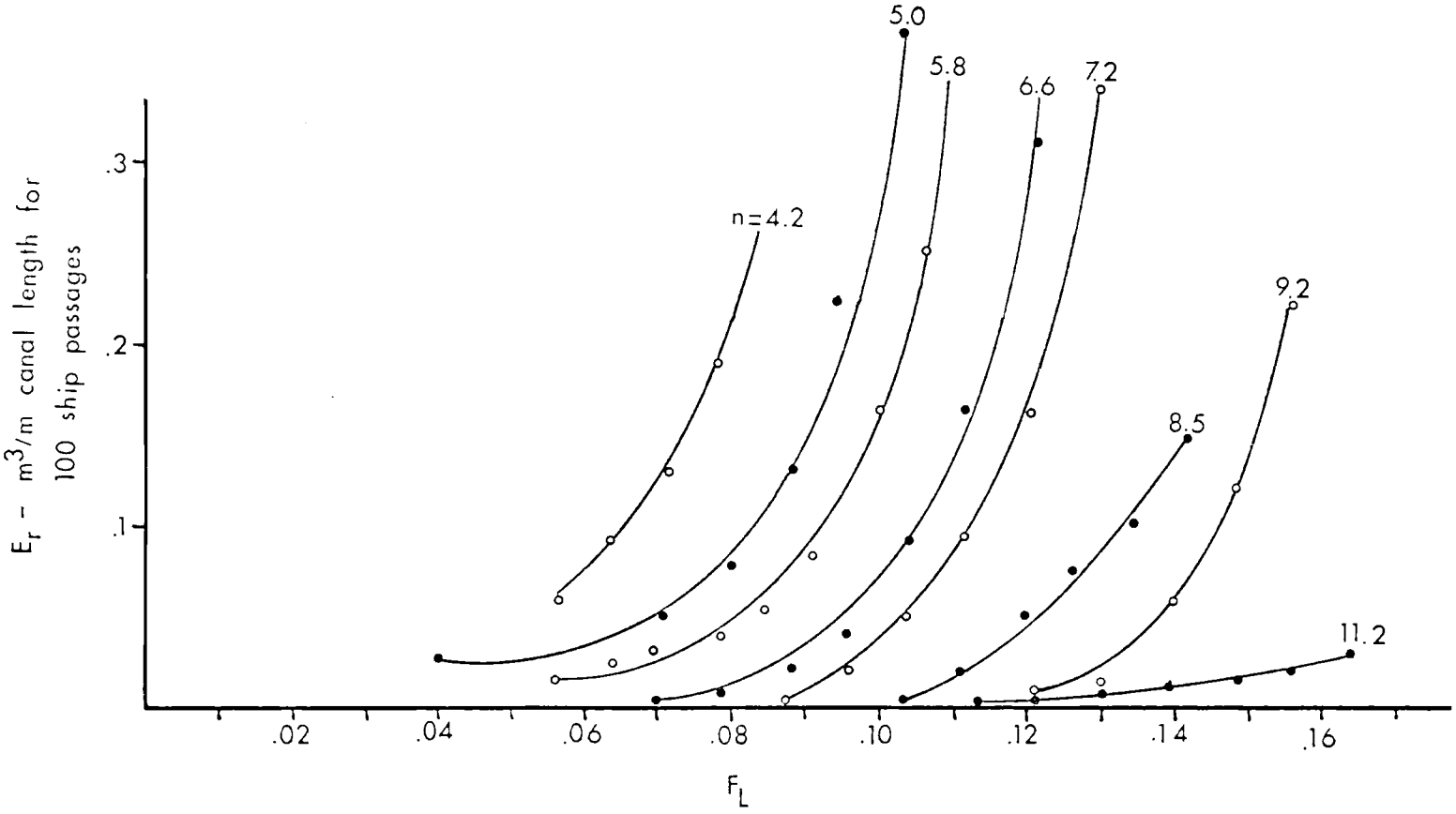


Figure 22. Rate of erosion in a canal for different passage coefficients. (Data from Wasser-und Schiffahrtsdirektion Kiel, 1966)

# VII. FIELD WORK

Field work concerned with determination of channel shipping impacts on benthic systems was carried out at Coos Bay, Oregon during 1974 to 1976 (Figure 23). Coos Bay is a world leader in the shipment of wood products with an average of 420 ships entering the port per year. The inner channel at Coos Bay is maintained to a depth of 9.1 meters and a width of 91.4 meters for 24.1 kilometers extending from the entrance to the mouth of Isthmus Slough. There are two turning basins in the harbor, one is opposite Coalbank Slough at Kilometer 23.5 and the other is at the City of North Bend at Kilometer 19.5. Both turning basins are maintained 9.1 meters deep, generally 183 meters wide, and 305 meters long (Coos Bay EIS Supplement, 1975).

The cargo vessels that come to Coos Bay can be arranged into three main classes. There are tankers, general-cargo vessels, and wood chip ships. With the channel depth limitations, tankers have been the older, smaller types such as T-1's and T-2's of 17,500 DWT and less. General-cargo vessels have been mostly C-1's, C-3's, Liberty, and Victory ships with a tonnage between 10,000 and 20,000 DWT. The dry-bulk carriers, moving wood chips, are new vessels in the 20 - 42,000 DWT range. The physical dimensions of the different classes of ships and the frequency of vessels calling at Coos Bay based on size are listed in the Appendix.

The objective of the field work was to determine the effect ship traffic has on the bottom sediments in a harbor. This was to be accomplished by determining the increase in velocity near the channel bot-

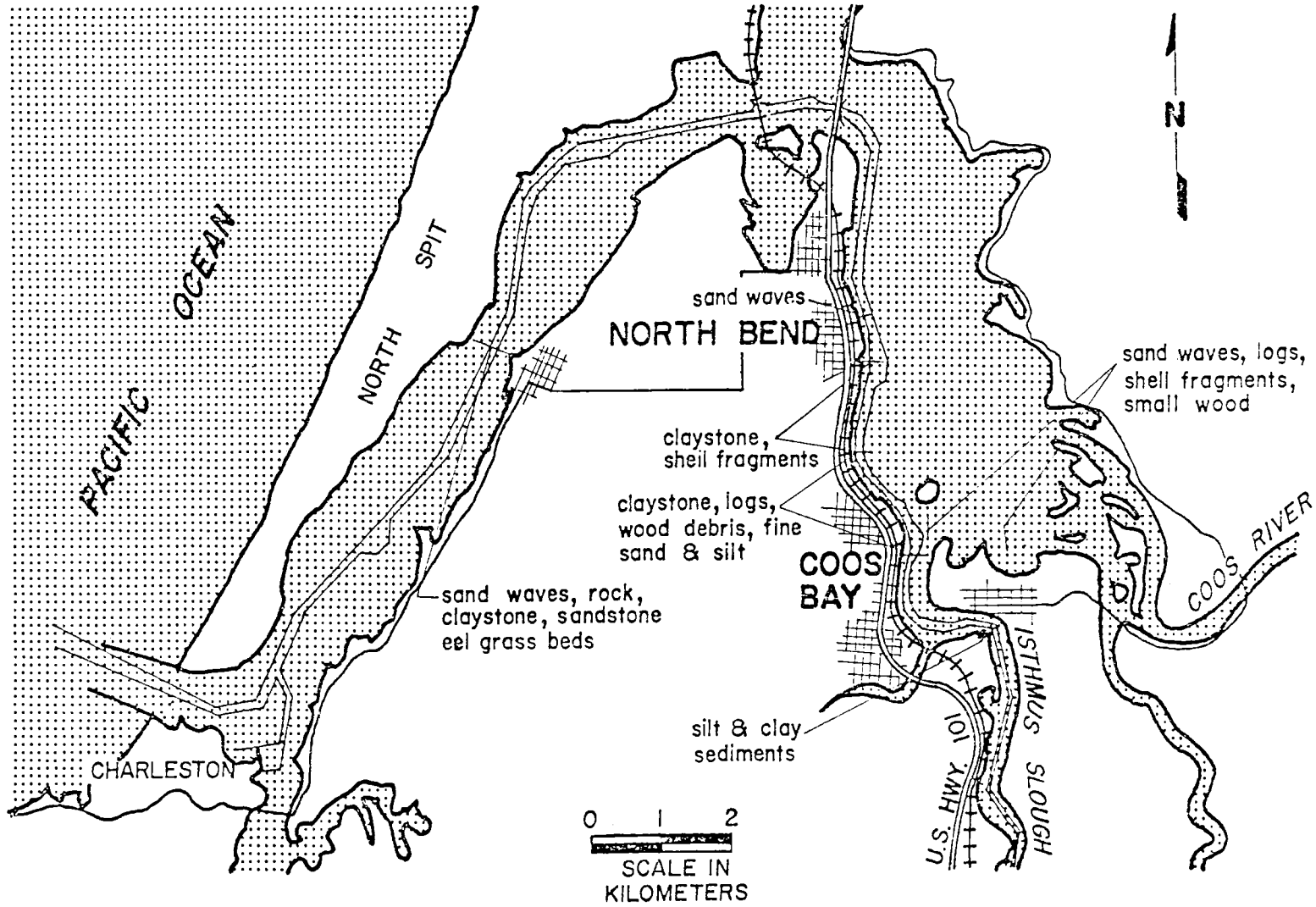


Figure 23. Chart of Coos Bay Estuary, Coos County, Oregon. (From Hartman, 1976)

tom caused by the presence of a ship and the ensuing increase in turbidity behind the ship. The research that was carried out was divided into four areas: 1) the velocity increase under a stationary ship; 2) the velocity increase under a moving ship; 3) the propeller wake; and 4) water quality (turbidity) behind a ship.

The field work at Coos Bay was performed in a straight section of the shipping channel adjacent to the U.S. Army Corps of Engineers' dock during the period June 1975 to January 1976. This location was chosen so the Corps dock could be used to store recording equipment. Adjacent to the Corps dock the channel bottom is composed mainly of silt, with the channel being 91.4 meters wide and having a Mean Low Water (MLW) depth of 11.6 meters at this location.

To determine the effect of a passing ship, a tripod (as shown in Figure 24) was built that would support instrumentation for determining: the current velocity at two elevations above the bottom and the current direction, and for collecting water samples in proximity to the bottom. Two Gurley 665 Direct Reading Current Meters were used to take velocity measurements. The sensing units were mounted one meter apart on the instrument stand. An electrical cable 92 meters long from the instrument stand to the Corps dock connected the current meters with the indicator unit. The meter face was calibrated to two different scales: 0-3 m/sec and 0-7 m/sec. The direction indicator showed which direction the water current was running; this was not designed to accurately determine the current direction, but mainly to record a reversal in the flow direction. Water samples were taken through a hose (1.5 cm inner diameter) that was supported between the current

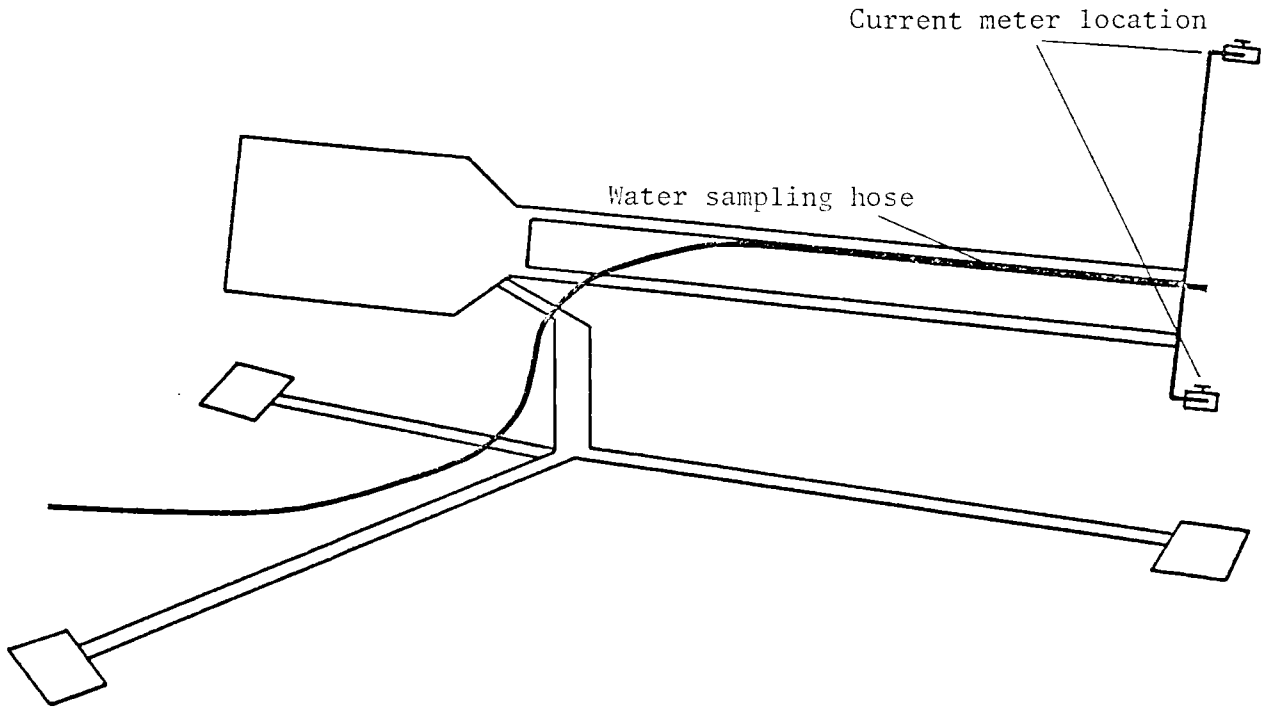


Figure 24. Schematic of instrument stand.

meters; one pump on the instrument stand and three Guppy pumps on the surface pumped the water to the dock where bottle samples were taken for water quality (turbidity) analysis.

The first experiment conducted was to determine if there was an increase in water velocity near the bottom due to the presence of a ship's hull. To accomplish this, the instrument stand was to be placed on the bottom under the center of a ship after it had docked. The Corps of Engineers hopper dredge the CHESTER HARDING was scheduled to be in port from June 21 - June 23, 1975, so the instrument stand was placed on the bottom in front of the Corps dock on June 20, 1975. Besides placing the instrument stand on the bottom, a Savonius current meter was put in downstream of the dock approximately the same distance out from the edge of the channel. It was intended to place the Savonius current meter sufficiently downstream to be away from induced currents associated with the HARDING. But unfortunately the HARDING tied up with its bow over the Savonius current meter and the resulting measurements had little meaning.

A different method for observing the effect of docked ships was to see if there was an increase in scour at a location where ships berth. Figure 25 shows a transect that was made parallel to Central Dock with a fathometer. The depth remains fairly constant in the area where ships normally berth. At each end of the dock the depth of water decreases. Since no special dredging is done in this area it can be assumed that the presence of the ships cause an increased scour velocity which removes the bottom sediments beneath the docked ships.

The subsequent field work consisted of measuring the water velo-

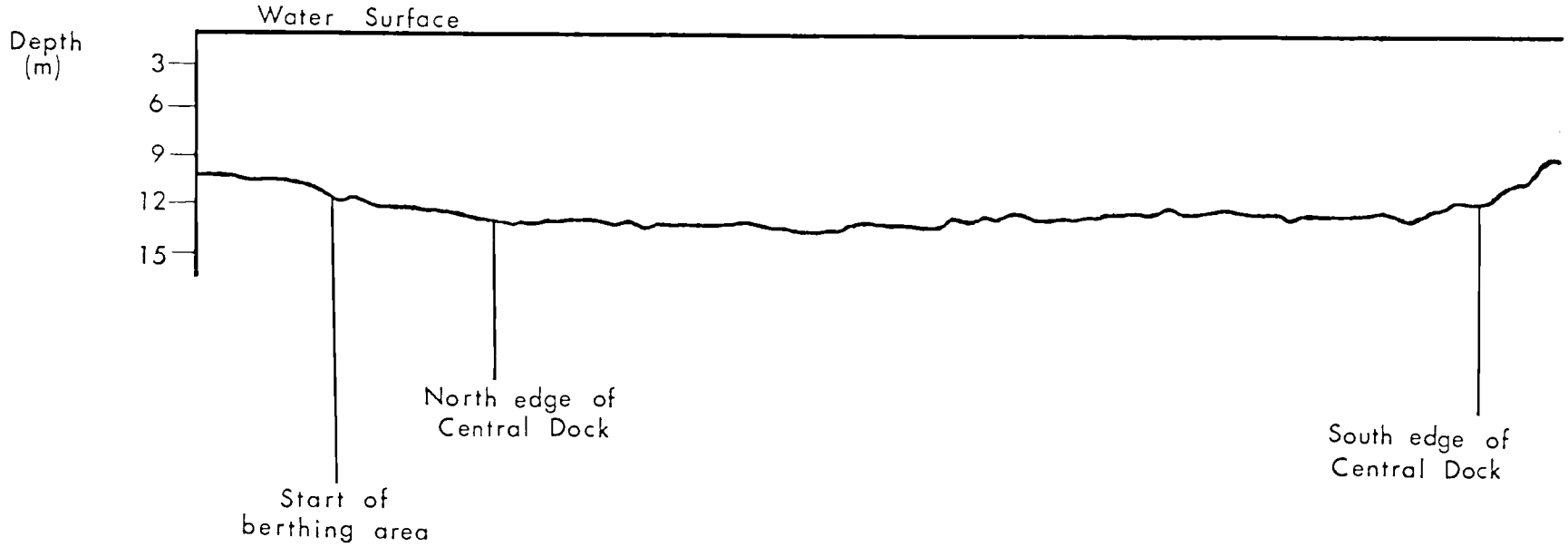


Figure 25. Bottom profile parallel to Central Docks, Coos Bay, Oregon.

city near the channel bottom as ships passed overhead. This was accomplished by placing the instrument stand on the centerline of the channel 46 meters directly out from the Corps dock. To put the instrument stand on the bottom required the use of an inflatable rubber boat and two divers. As the support craft proceeded out in the channel, dive weights were tied on the cable approximately every six meters as the cable was being pulled from the support reel. At the center of the channel the instrument stand was lowered to the bottom and then the divers proceeded to put lead weights on the legs to keep the stand in place.

The instrument stand was placed in the channel on July 10, 1975 with the intention of leaving it in place for two weeks to monitor the ship traffic that took place during that period of time. However, only five ships passed over the instrument stand before it was destroyed by a ship's anchor on July 12 and lost. Only a small amount of data was obtained from these ship passages. It was found that the velocity changed very quickly during ship passage and the output of the Gurley meters did not give adequate response to describe or record the velocity change associated with ship passage. Data that were obtained are summarized in Table III.

TABLE III. VELOCITY MEASUREMENTS AT COOS BAY

| Ship | Draft | Water Depth | Velocity change from free stream m/sec | | | |
|---|---|---|---|---|---|---|
| | m | m | Bow | Middle | Stern | Wake |
| Bunga Tembusa | 8.8 | 12.5 | 0.3 | 0.61 | 0.0 | 0.3 |
| Paragon | 3.7 | 11.3 | 0.0 | 0.43 | 0.3 | 0.0 |
| Yue Man | 4.0 | 11.3 | 0.0 | 0.80 | 1.2 | 0.0 |
| Daiko Maru | 5.4 | 12.0 | 0.0 | 0.90 | 0.2 | 0.0 |
| Septa | 6.9 | 12.5 | 0.0 | 0.20 | 0.3 | 0.2 |

The current meters that were destroyed were replaced with two Marsh McBirney Model 711 Electromagnetic Current Meters (EMCM). These meters are more accurate for rapid fluctuations in the current velocity and they were hooked up to a magnetic tape recorder to provide a permanent record of the data. On receipt of this equipment the meters were mounted as shown in Figure 26. The installation procedure was the same as for the instrument stand, except in this case one of the meters was put on the centerline of the channel and the other was placed approximately nine meters to the side of the channel centerline.

The current meters were placed in the channel on November 1, 1975. An acoustic pinger was fastened to the stand of the meter on the centerline of the channel to aid in recovery of the meter in case of another ship related accident. Shortly before the Bunga Melawis arrived on November 2, a float marking the location of the second current meter was pulled up. The anchor to the float hooked the current meter cable and tipped the current meter on its side. When the data from the remaining meter was analyzed, it was determined that an outside source was interfering with the current meter. The acoustic pinger was found

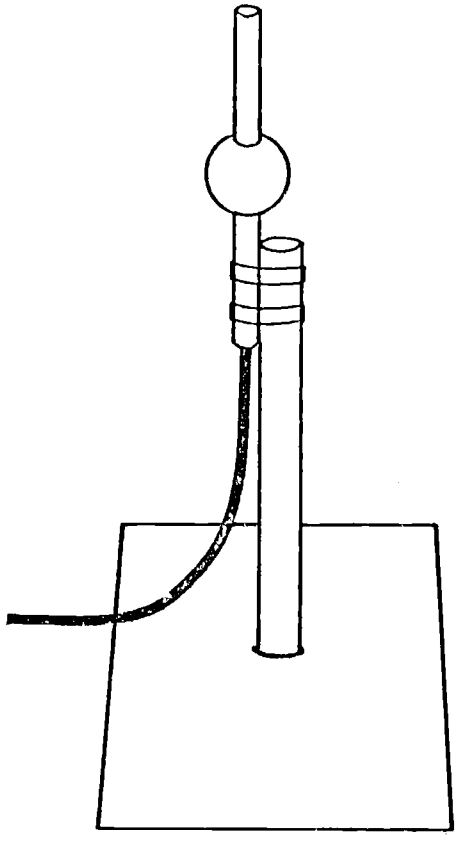

Figure 26. Mounting arrangement of electromagnetic current meters.

to produce a signal that interfered with the current meter, so the data collected could not be used.

To further isolate the meters, wooden stands were built for the next field trip from January 29 to February 4, 1976. Two ships passed over the stands coming into the harbor and two ships went over leaving the harbor. Again, some outside noise source interfered with the current meters to make the data unusable. Perhaps stray currents from the ships fathometers negated the current meter data collected. No further measurements of this sort were attempted.

The third area of the field work involved trying to determine the depth of the propeller wake behind a ship. The ship chosen to do the work behind was the dredge HARDING because it would be moving at a very slow speed (one to two knots) while it was dredging. The electromagnetic current meter with a spherical probe was attached to a vane with a weight attached to keep it oriented into the current. It was hoped to lower the current meter down to record when it was below the wake, but the current in the wake was so strong that it pushed the meter backwards at a 30° angle from the surface. Using this procedure it was not possible to tell how deep the propeller wake extended.

Water samples that were collected in July and October 1975 and January 1976 were analyzed to determine the turbidity of the water. The water samples with the first instrument stand were collected at a height one meter off the bottom by pumping water to the surface through a hose. After the instrument stand was destroyed, Van Dorn bottles were used to collect water samples at 1.5, 6.1 and 10.7 meters below the surface. Water samples were collected over both sandy and silty

bottoms. The samples were analyzed with a HACH Laboratory Turbidimeter Model 1860A. It was found that there was no observable increase in turbidity due to the passage of a ship.

# VIII. SEDIMENT TRANSPORT IN COOS BAY

## Estimate of Ship Induced Erosion

Although the field tests did not give an indication of any substantial influence that ship traffic has on the sediment transport in the Coos Bay channel, some further discussion will be made on this subject. The field tests were not designed to measure the sediment transport outright, but to determine if erosion existed through velocity measurements and water samples. In order to comment on the approximate sediment transport caused by ship traffic, results of the SOGREAH tests (Figure 22) have been extended for conditions at three sections of the Coos Bay channel. The three sections were chosen where there were data on the sediment deposition in the channel. From this information, the predicted erosion due to ship traffic can be compared to the natural erosion.

The channel at Coos Bay is composed of several different types of sediment. The sediment of lower Coos Bay, from the entrance to the Highway 101 bridge, is predominantly sand. From the Highway 101 bridge to approximately Kilometer 16.9 the bottom consists of a large amount of shell deposits. From Kilometer 16.9 to Kilometer 20.1 the bottom is silt. For the next several hundred meters the bottom is rock, hard clay, and silt. The bottom then returns to mainly silt at Kilometer 21.9 (Coos Bay EIS Supplement, 1975). The median grain size for the estuary is 0.2 mm to 0.3 mm with the exception of the silt which ranges in size from .015 mm to .02 mm. During periods of high runoff the median grain size in some areas can range from .48 mm to

.55 mm (Arneson, 1975). The range in grain size in most of Coos Bay is similar enough to the canals studies in the SOGREAH tests that it is believed the results of the SOGREAH tests (Figure 22) can be used to estimate the erosion caused by ship traffic in Coos Bay. The only area where the SOGREAH results would be inaccurate would be the regions of the Coos Bay canal composed of silt.

The number of vessels that used Coos Bay in 1975 can be arranged in three categories: 315 dry cargo ships, 23 tankers, and 92 barges. The largest dimensions for these types of vessels are listed in Table IV.

TABLE IV. CHARACTERISTICS OF SHIPS IN COOS BAY

| Vessel | Length m | Beam m | Draft m | No/Year |
|---|---|---|---|---|
| Dry Cargo | 217.0 | 32.3 | 9.1 | 315 |
| Tanker | 201.5 | 27.4 | 9.1 | 23 |
| Barge | 73.2 | 18.3 | 4.0 | 92 |

The vessels usually travel at speeds from 14.8 to 16.7 km/hr from the entrance to the Highway 101 bridge, while above the bridge the vessels usually travel at 3.7 to 5.6 km/hr.

The shipping canal at Coos Bay is maintained to a depth of 9.1 meters and a width of 91.4 meters with a side slope of one to three. In reality, the canal is much larger than the maintained canal. The value of n, the ratio of the canal cross-sectional area to the maximum ship cross-sectional area, for three sections of the canal are listed in Table V.

TABLE V. ESTIMATED EROSION FOR 100 SHIP PASSAGES[3]

| | Values of n and $E_r$ $m^3/m$ | | | | | | |
|---|---|---|---|---|---|---|---|
| | Dry Cargo | | Tanker | | Barge | | Total Erosion |
| | n | $E_r$ | n | $E_r$ | n | $E_r$ | $m^3/km$ |
| Entrance | 9.1 | 0 | 10.7 | .001 | 36.9 | 0 | .23 |
| Kilometer 9.8 | 12.5 | 0 | 14.7 | 0 | 50.8 | 0 | 0 |
| Kilometer 21 | 5.1 | .025 | 6.0 | .015 | 20.9 | 0 | 82.2 |

Also listed in Table V is the estimated erosion that each ship would cause in 100 ship passages and the total erosion over a year for a section of the canal one kilometer long in each of the three regions. Table V shows that the critical area for erosion is in the upper portion of the bay which is also the region where the SOGREAH test results are not as applicable because of the silt in the canal.

In addition to the erosion caused during a ship passage, a considerable amount of erosion occurs when a ship drags its anchor. Hartman (1976) has calculated that approximately 350,000 cubic meters of bottom sediments are disturbed annually by ship anchor dragging from Kilometer 19.3 to 24.6. For the same section of the canal, the estimated erosion due to ship traffic is only 436 $m^3$/year. The main reason that the scour from the anchors is much greater than the scour from a ship passage is the way in which the two quantities are defined. In the SOGREAH test the erosion was determined by the quantity of material that was transported and deposited in the center of the canal. Hartman (1976) determined the quantity of sediment that would be disturbed by an anchor but not necessarily eroded. Most of the sediment

[3]Taken from Figure 22; SOGREAH, 1966.

disturbed by an anchor remains in the same location with only the fine material being put in suspension.

Natural Deposition in River

The best estimate of the total deposition that occurs in the canal over a year is the amount of material that is dredged each year to maintain the canal at its proper dimensions. Data on the deposition in three reaches of the canal was obtained from the Army Corps of Engineers and averaged over a three year period to get a yearly average for each section. At the entrance the yearly deposition is 413 $m^3/m$ canal length. By Kilometer 9.7 the deposition is 13 $m^3/m/year$, while near the Corps dock the deposition rate is about 86 $m^3/m/year$. The different rates of deposition are caused by the different sources and transport of sediment near each location.

The sources of sediment at Coos Bay include the ocean and the rivers and streams which empty into the estuary. There is also a substantial amount of material that comes from the erosion of tidal flats and spoil islands by wave action, materials disturbed by dredging, and particles blown into the estuary by the wind (Ippen, 1966 and Slotta et al. 1973). Near the entrance the main portion of the sediment is brought into the estuary by the littoral drift. The sediment is usually sand of the same type as found on nearby beaches (Kulm and Byrne, 1966). Near the city of Coos Bay the majority of the deposition would by due to the inflow of sediment from the Coos River. Approximately 72,000 tons of sediment comes into Coos Bay each year from the rivers (Arneson, 1975). In comparison to the large amount of sediment trans-

port that occurs naturally, the ships seem to contribute a very insignificant part to the total sediment transport.

# IX. CONCLUSIONS AND RECOMMENDATIONS

Ship traffic in confined waters can lead to serious erosion of the canal banks and sides under certain conditions. The two most important factors that influence the erosion are the ship speed and the ratio of the canal cross-sectional area to the maximum ship cross-sectional area. In Coos Bay, Oregon it was found that the erosion caused by ship traffic (excluding anchor dragging) is insignificant compared to the annual sediment transport from natural causes.

In dredging future navigation canals, the SOGREAH test results (Figure 22) can be used to estimate the amount of erosion in a proposed canal to help determine the optimum size of canal based on initial construction costs and maintenance dredging costs. The SOGREAH test results can be used with reasonable accuracy for canals with a median grain size between 0.2 and 0.7 mm. More research is needed though on the erosion caused by ships in canals composed of silt or cohesive sediments.

# X. BIBLIOGRAPHY

Adee, Bruce H., "Calculation of the Streamlines About A Ship Assuming A Linearized Free-Surface Boundary Condition," Journal of Ship Research, Vol. 17, No. 3, Sept. 1973, pp. 140-146.

Anderson, Franz E., "The Effect of Boat Waves on the Sedimentary Processes of a New England Tidal Flat," Department of Earth Sciences and Jackson Estuarine Laboratory, University of New Hampshire, Durham, New Hampshire, 1974, Technical Report No. 1.

Arneson, R.J., Seasonal Variations in Tidal Dynamics, Water Quality, and Sediments in the Coos Bay Estuary, M.Oc.E. Thesis, Department of Civil Engineering, Oregon State University, Corvallis, Oregon, 1975.

Beck, R.F., Newman, J.N. and Tuck, E.O., "Hydrodynamic Forces on Ships in Dredged Channels," Journal of Ship Research, Vol. 19, No. 3, Sept. 1975, pp. 166-171.

Breslin, J.P. and Tsakonas, S., "The Blade Frequency Velocity Field Near an Operating Marine Propeller Due to Loading and Thickness Effects," 6th Midwestern Conference on Fluid Mechanics, 1959.

Constantine, T., "On the Movement of Ships in Restricted Waterways," Journal of Fluid Mechanics, Vol. 9, October 1960, pp. 247-257.

Das, M.M. and Johnson, J.W., "Waves Generated by Large Ships and Small Boats," Proceedings of the Twelfth Coastal Engineering Conference, Sept. 1970, Washington, D.C., pp. 2281-2286.

Delft Hydraulics Laboratory, Anantasting van dworsprofielen in vaarwegen, Schelde-Rijnverbinding, M 1115, deel 1A, 1B, Dec. 1974.

Denny, Stephen B., "Applicability of the Douglas Computer Program to Hull Pressure Problems," Hydromechanics Laboratory Research and Development Report No. 1786, Dept. of the Navy, Oct. 1963.

Draft Supplement, Coos Bay, Oregon Deep Draft Navigation Project Environmental Impact Statement, Vol. I & II, U.S. Army Engineer District, Portland, Oregon, Feb. 1975.

"Druck und Stromung unter im Kanal fahrenden Schiffen," Kriegenbrunner Messungen, Schiff und Hafen, Vol. 8, 1973, pp. 691-696.

Felkel, Karl and Steinweller, Heiko, "Natur und Modellversuche Uber Die Wirkung Der Schiffe Auf Flussohlen Aus Grobkies," Wasserwirtschaft, Vol. 62, No. 8, Aug., 1972, pp. 243-249.

Hansen and Davis, Personal Communication with Author, Oct. 1975.

Harsha, P.T., "Free Turbulent Mixing, a Critical Evaluation of Theory and Experiment," Arnold Engineering Development Center, Arnold Air Force Station, Tenn., AD718956, Feb. 1971.

Hart, E.D., Radioactive Sediment Tracer Tests Houston Ship Channel, Houston, Texas, Miscellaneous Paper H-69-2, March, 1969, Sponsored by U.S. Army Engineer District, Galveston, Texas.

Hartman, Greg, Evaluation of Estuarine Channel Conditions In Coos Bay, Oregon Using Side Scan Sonar, M.S. Thesis presented to Oregon State University, Corvallis, Oregon, 1976, in partial fulfillment of the requirements for the degree of Master of Science.

Hess, John L. and Smith, A.M., "Calculation of Nonlifting Potential Flow About Arbitrary Three-Dimensional Bodies," Journal of Ship Research, Sept., 1964, pp. 22-44.

Ippen, A.T., "Sedimentation in Estuaries," Estuary and Coastline Hydrodynamics, A.T. Ippen, ed., Chap. 15, McGraw-Hill, New York, N.Y., 1966.

Karaki, S. and van Hoften, J., "Resuspension of Bed Material and Wave Effects on the Illinois and Upper Mississippi Rivers Caused by Boat Traffic," prepared for the U.S. Army Engineer District, St. Louis, Contract No. LMSSD 75-881, June, 1975.

Kray, Casimir J., "Supership Effect on Waterway Depth and Alignments," Journal of the Waterways and Harbors Division, ASCE, May, 1970, pp 497-530.

Kulm, L.D. and J.V. Byrne, "Sedimentary Response to Hydrography in an Oregon Estuary," Marine Geology, Vol. 4, No. 2, 1966.

Maxwell, W., and Paywash, H., "Axisymmetric Shallow Submerged Turbulent Jets," Journal of the Hydraulics Division, ASCE, April, 1973, pp.637-652.

Murray, Stephen P., "Settling Velocities and Vertical Diffusion of Particles in Turbulent Water," Journal of Geophysical Research, Vol. 75, No. 9, March, 1970, pp. 1647-1654.

Namimatsu, Masaaki and Muroaka, Jenji, "Wake Distribution of Full Form Ship," IHI Engineering Review, Vol. 7, No. 3, Sept., 1974, Ishikawajima Harima Heavy Industries Co., Ltd., Japan.

Physics of Sound in the Sea, Dept. of the Navy, Headquarters Naval Material Command, Washington, D.C., 1969, p. 566.

Plotkin, Allen, "Flow Past an Anchored Slender Ship in Variable-Depth Shallow Water: An Extension," to appear in Journal of Hydronautics, Jan., 1976.

Plotkin, Allen, Flow Past an Anchored Slender Ship in Variable-Depth Shallow Water," Journal of Hydronautics, Vol. 9, No. 7, July, 1975, pp. 103-106.

Port Commissioner, Coos Bay, Oregon, Personal Communication with Author, Jan., 1976.

Saunders, Harold E., Hydrodynamics in Ship Design, Vol. I, The Society of Naval Architects and Marine Engineers, New York, N.Y., 1957, p. 739.

Schiffbau, "Versuche zur Feststellung des schädlichen Einflusses der Schiffsschrauben auf die Kanalsohle und Mittel zur Beseitigung beziehungsweise Verminderung desselben," No. 23, Sept. 11, 1912, pp. 948-959.

Schofield, R. Bryan, "Speed of Ships in Restricted Navigation Channels," Journal of the Waterways, Harbors and Coastal Engineering Division, ASCE, May, 1974, pp. 133-150.

Slotta, L.S. et al., "Effects of Hopper Dredging and In Channel Spoiling in Coos Bay," Oregon State University, Corvallis, Oregon, 1973.

Slotta, L.S. and Montes, J.S., "Dredging by Means of Water Jets," 1975, Oregon State University, unpublished.

Sorensen, R.M., "Waves Generated by a Moving Ship," Shore and Beach, Vol. 35, No. 1, April, 1967, pp. 21-25.

Streeter, Victor L., Fluid Mechanics, Fourth edition, McGraw-Hill Book Co., New York, N.Y., 1966, pp. 134-139.

Tuck, E.O., "Shallow-Water Flows Past Slender Bodies," Journal of Fluid Mechanics, Vol. 26, 1966, pp. 81-95.

Tuck, E.O. and Taylor, P.J., "Shallow-Wave Problems in Ship Hydrodynamics," presented at the Eighth Symposium in Naval Hydrodynamics at Pasadena, Cal., Aug., 1970, pp. 627-657.

Wasser-und Schiffahrtsdirektion Kiel: Rahmenentwurf Sicherung des Nord-Ostall-Kanals, Bericht 2, Bemessung des Kanalquerschnitts, Modellversuche der SOGREAH, Band 1 und 2, 1966, unpublished.

Waugh, Jr., Richard G., "Water Depths Required for Ship Navigation," Journal of the Waterways, Harbors, and Coastal Engineering Division, ASCE, Aug., 1971, pp. 455-473.

# XI. APPENDIX

Classes and Characteristics of Vessels Calling at Coos Bay

| Type & Class | DWT | length m | beam m | draft m | speed km/hr |
|---|---|---|---|---|---|
| General Cargo | | | | | |
| Liberty | 10,800 | 134.6 | 17.9 | 8.4 | 20.4 |
| Victory | 10,800 | 138.8 | 18.9 | 8.7 | 31.5 |
| C-2 | 10,500 | 134.0 | 19.2 | 8.2 | 28.7 |
| C-3 | 12,300 | 150.0 | 21.2 | 9.0 | 30.6 |
| C-4 | 13,600 | 174.3 | 22.9 | 9.6 | 37.0 |
| C-4 converted | 15,000 | 159.3 | 21.8 | 10.0 | 31.5 |
| Star Steamship | 29,240 | 171.9-182.9 | 22.9-25.9 | 10.7-11.2 | 29.6 |
| Tanker | | | | | |
| T-2 | 17,000 | 160.0 | 21.3 | 9.1 | 26.9 |
| T-2 jumboized | 21,000 | 178.0 | 24.4 | 9.9 | 27.8 |
| T-5 | 26,000 | 196.6 | 25.9 | 10.1 | 29.6 |
| | 35,000 | 201.5 | 27.4 | 10.9 | 33.3 |
| Bulk Carrier | | | | | |
| Chip ship | 20,700 | 178.3 | 21.9 | 9.5 | 27.8 |
| Chip ship | 27,400 | 194.6 | 25.2 | 10.5 | 27.8 |

Taken from Coos Bay E.I.S. Supplement, 1974.

Number of Vessels Calling at Coos Bay 1956-1975

| Year | Vessel Draft (m) 6.4-7.3 | 7.6-8.5 | 8.5-9.1 | 9.1+ | Total |
|---|---|---|---|---|---|
| 1956 | 84 | 67 | 107 | 4 | 262 |
| 1957 | 180 | 65 | 93 | 11 | 349 |
| 1958 | 178 | 80 | 72 | 10 | 340 |
| 1959 | 189 | 116 | 79 | 6 | 390 |
| 1960 | 208 | 106 | 98 | 15 | 427 |
| 1961 | 175 | 106 | 69 | 13 | 363 |
| 1962 | 187 | 75 | 65 | 23 | 351 |
| 1963 | 183 | 95 | 70 | 16 | 363 |
| 1964 | 164 | 100 | 62 | 23 | 349 |
| 1965 | 206 | 80 | 78 | 15 | 379 |
| 1966 | 227 | 97 | 75 | 37 | 436 |
| 1967 | 277 | 106 | 134 | 33 | 550 |
| 1968 | 294 | 146 | 179 | 30 | 650 |
| 1969 | | | | | 398 |
| 1970 | | | | | 394 |
| 1971 | | | | | 324 |
| 1972 | | | | | 393 |
| 1973 | | | | | 394 |
| 1974 | | | | | 455 |
| 1975 | | | | | 430 |

1956-1968 from Coos Bay EIS Supplement, 1975

1969-1975 Personal communication by author with Port Commission, Coos Bay, Oregon.

## Kriegenbrunner Surveys

Motor-freight ship

| | |
|---|---|
| length | 85 m |
| width | 9.5 m |
| draft | 2.3 m |
| propeller diameter | 1550 mm |

Tugboat

| | |
|---|---|
| length | 25.5 m |
| width | 10.8 m |
| draft | 1.65 m |

Barge

| | |
|---|---|
| length | 76.5 m |
| width | 11.4 m |
| draft | 2.3 m |

Different water depths in canal

4.0 m
3.5 m
3.1 m
2.8 m

## Breisacher Versuche (Felkel and Steinweller, 1972)

Gustav Koenigs

| | |
|---|---|
| length | 67 m |
| width | 8.2 m |

4 bladed propeller 1.47 m diameter

## Results of Kriegenbrunner Survey

| 1 | 2 | 3 | 4 | 5 | 6 | 7 | 8 |
|---|---|---|---|---|---|---|---|
| 1.40.1 | 2.71 | -0.06 | 0.45 | -3.50 | 1.71 | | 14.68 |
| 1.40.2 | 3.12 | -0.85 | 0.45 | -4.20 | 1.60 | | 19.00 |
| 1.40.3 | 3.41 | -0.95 | 0.65 | - | 1.46 | 8.06 | 21.65 |
| 1.40.4 | 3.57 | -0.95 | 0.75 | - | 1.32 | | 23.35 |
| 1.40.5 | 3.42 | -1.15 | 0.90 | - | 1.12 | | |
| 2.40.1 | 2.21 | -0.65 | - | -2.95 | 1.77 | | 10.75 |
| 2.40.2 | 2.72 | -0.85 | 0.80 | -1.95 | 1.69 | | 14.10 |
| 2.40.3 | 2.94 | -0.85 | 0.55 | - | 1.57 | 6.76 | 16.20 |
| 2.40.4 | 2.99 | -1.20 | - | - | 1.43 | | 17.55 |
| 2.40.5 | 3.09 | -1.10 | 1.10 | - | 1.26 | | 18.00 |
| 1.35.1 | 2.48 | -0.75 | 0.55 | -2.50 | 1.17 | | 14.68 |
| 1.35.2 | 3.03 | -0.95 | 0.85 | -1.40 | 1.00 | | 18.65 |
| 1.35.3 | 3.03 | -1.10 | 1.00 | -1.70 | 0.91 | 6.70 | 21.65 |
| 1.35.4 | 2.97 | -1.20 | 1.00 | -1.10 | 0.76 | | 22.65 |
| 1.35.5 | 3.04 | -1.15 | 1.00 | 0 | 0.58 | | 23.80 |
| 2.35.1 | 2.09 | -0.85 | - | - | 1.19 | | 10.90 |
| 2.35.2 | 2.43 | -1.30 | 0.95 | - | 0.06 | | 14.10 |
| 2.35.3 | 2.69 | - | 1.50 | -2.00 | 0.92 | 5.61 | 16.18 |
| 2.35.4 | 2.57 | -1.30 | 2.20 | -1.70 | 0.85 | | 17.43 |
| 2.35.5 | 2.68 | -1.20 | 1.60 | -0.55 | 0.59 | | 18.03 |
| 1.31.1 | 2.36 | -0.75 | 0.35 | -1.95 | 0.80 | | 14.33 |
| 1.31.2 | 2.59 | -1.05 | 0.65 | -1.95 | 0.71 | | 18.33 |
| 1.31.3 | 2.66 | -1.30 | - | -1.95 | 0.65 | 5.77 | 20.65 |
| 1.31.4 | 2.75 | -1.15 | 1.20 | -2.10 | 0.53 | | 22.00 |
| 1.31.5 | 2.72 | -1.15 | 1.30 | +0.70 | 0.26 | | 23.00 |
| 2.31.1 | 1.90 | -0.95 | 0.80 | -1.80 | 0.77 | | 10.73 |
| 2.31.2 | 2.34 | -1.70 | 1.40 | -0.30 | 0.48 | | 14.12 |
| 2.31.3 | 2.32 | -1.40 | 1.80 | +0.20 | 0.32 | 4.83 | 16.10 |
| 2.31.4 | 2.31 | -1.40 | 2.30 | -0.40 | 0.18 | | 17.15 |
| 2.31.5 | 2.35 | -1.30 | 2.65 | 0 | 0.05 | | 17.90 |
| 2.28.1 | 1.84 | -1.10 | 1.50 | -1.00 | 0.49 | | 10.75 |
| 2.28.2 | 2.09 | -1.70 | 2.10 | -1.00 | 0.30 | | 14.05 |
| 2.28.3 | 2.13 | -1.80 | - | -1.40 | 0.05 | 4.39 | 16.37 |
| 2.28.4 | 2.15 | - | - | -1.25 | 0.02 | | 17.53 |

1. Test number
2. Ship speed above the bottom (m/sec)
3. Maximum return current under bow (m/sec)
4. Maximum following current (m/sec)
5. Deviation of ship from center of channel (m)
6. Clearance between moving ship and bottom (m)
7. Passage coefficient, n
8. Propeller frequency (HZ)